Results and Prospects of LHAASO Cosmic Ray Composition and Energy Spectra Measurement

Shoushan Zhang

on behalf of the LHAASO collaboration

Institute of High Energy Physics，CAS，China

The 9th Roma International Conference on Astro-Particle Physics (RICAP-2024)
23 - 27 September., 2024 Roma, Italy

Outline

- Introduction
- CR Spectra around the Knees
  - Pure Protons
  - Light Component (H + He)
  - All Particle Spectrum and Composition
- Summary & Outlook

Cosmic rays

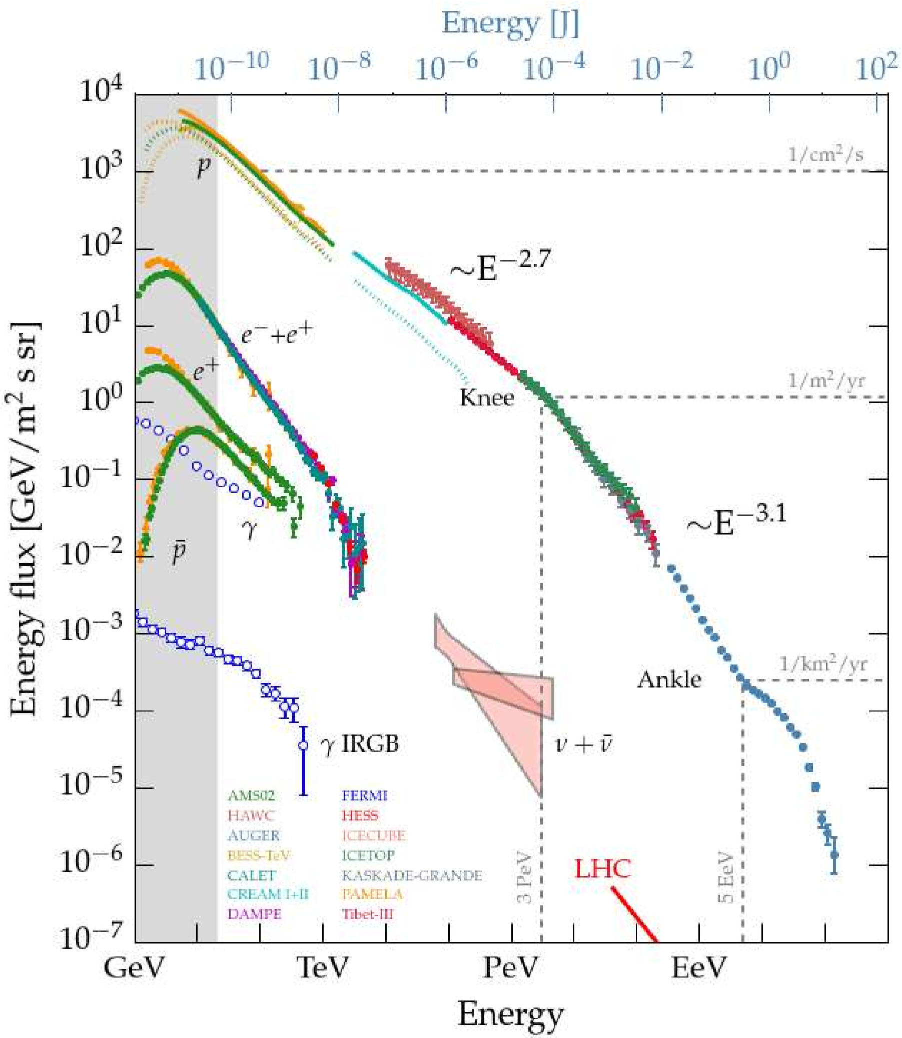

C.Evoli 10.5281/zenodo.1468853

- Proton, helium nuclei and heavier nuclei , all the way to uranium
- Discovered in 1912, many things (e.g. source, acceleration mechanism) about cosmic rays remain a mystery more than a century later
- Individual energy spectra play am important role to solve the mystery
  - Proton knee, helium knee, iron knee …
  - The knee indicates the energy limit for cosmic ray acceleration by astrophysical sources.

- **KASCADE experiment**
  - **Altitude： 110m**
  - **Unfolding： μ and electron matrix**
  - **The results strongly depend on the hadronic interaction models**
- **Individual components of CRs energy spectrum measurement are very important, but not easy.**

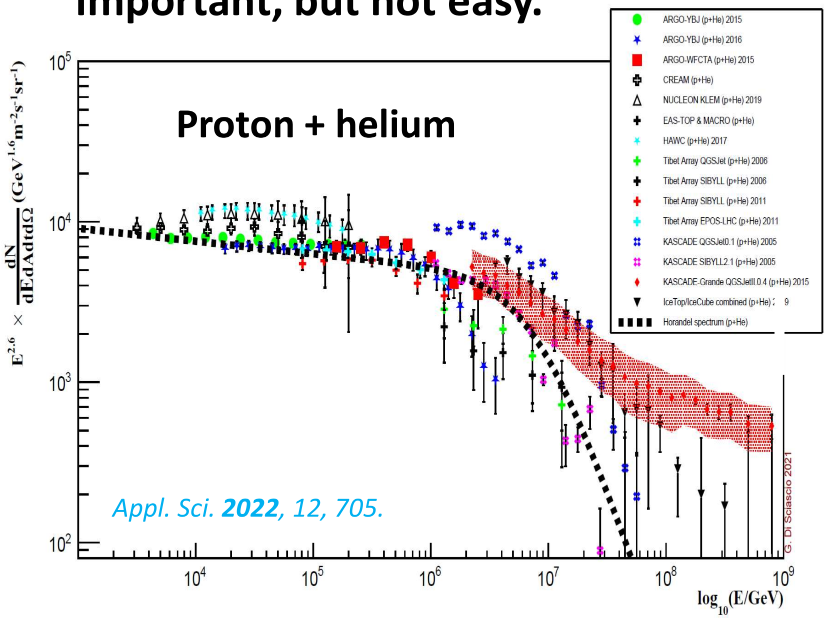

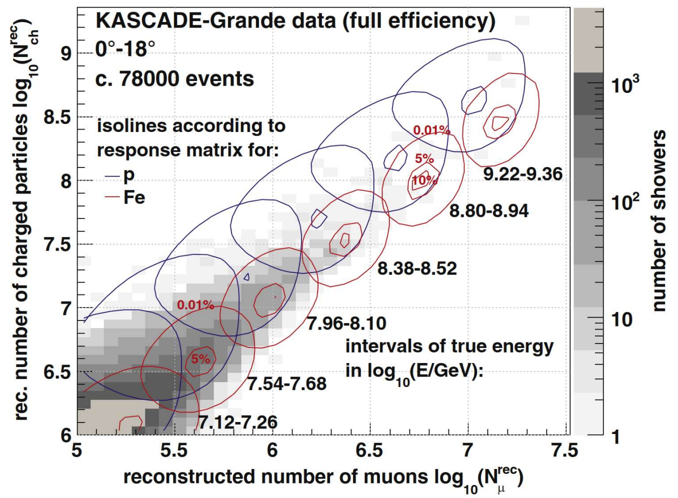

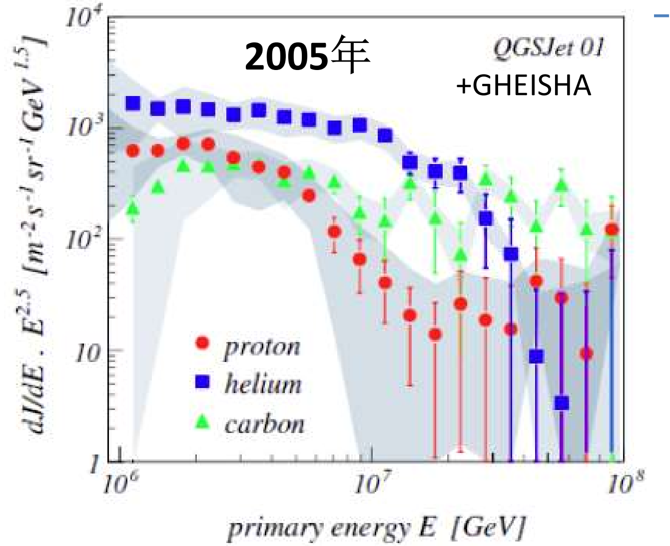

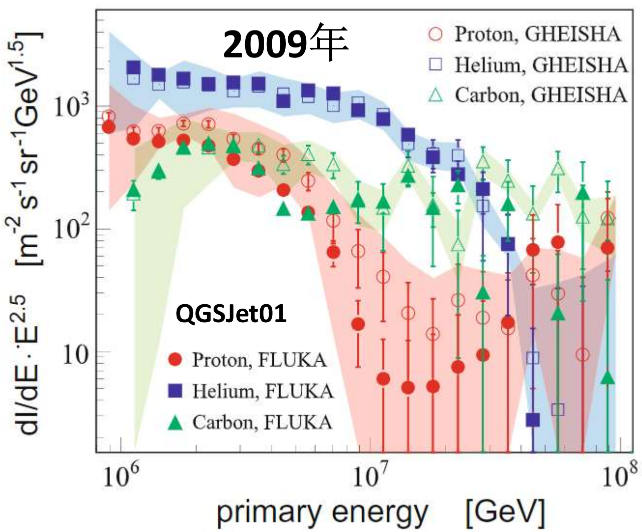

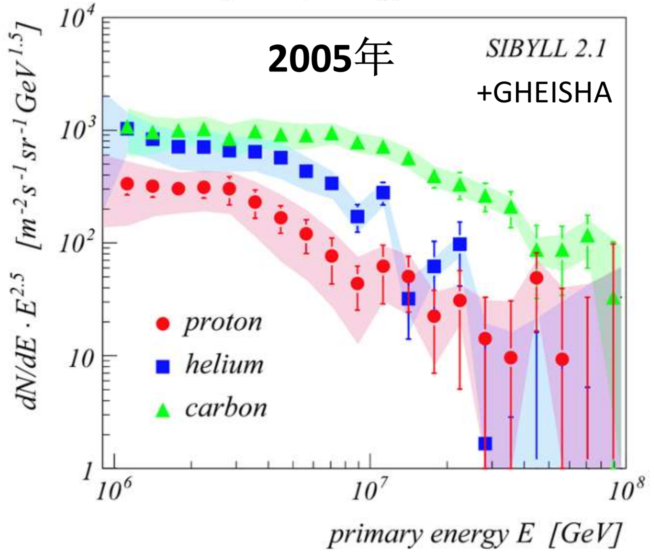

High Energy Cosmic Rays

Large High Altitude Air Shower Observatory (LHAASO)

LHAASO Physics Topics

- Gamma Ray Astronomy
- Charged CRs measurement
- New Physics Frontier

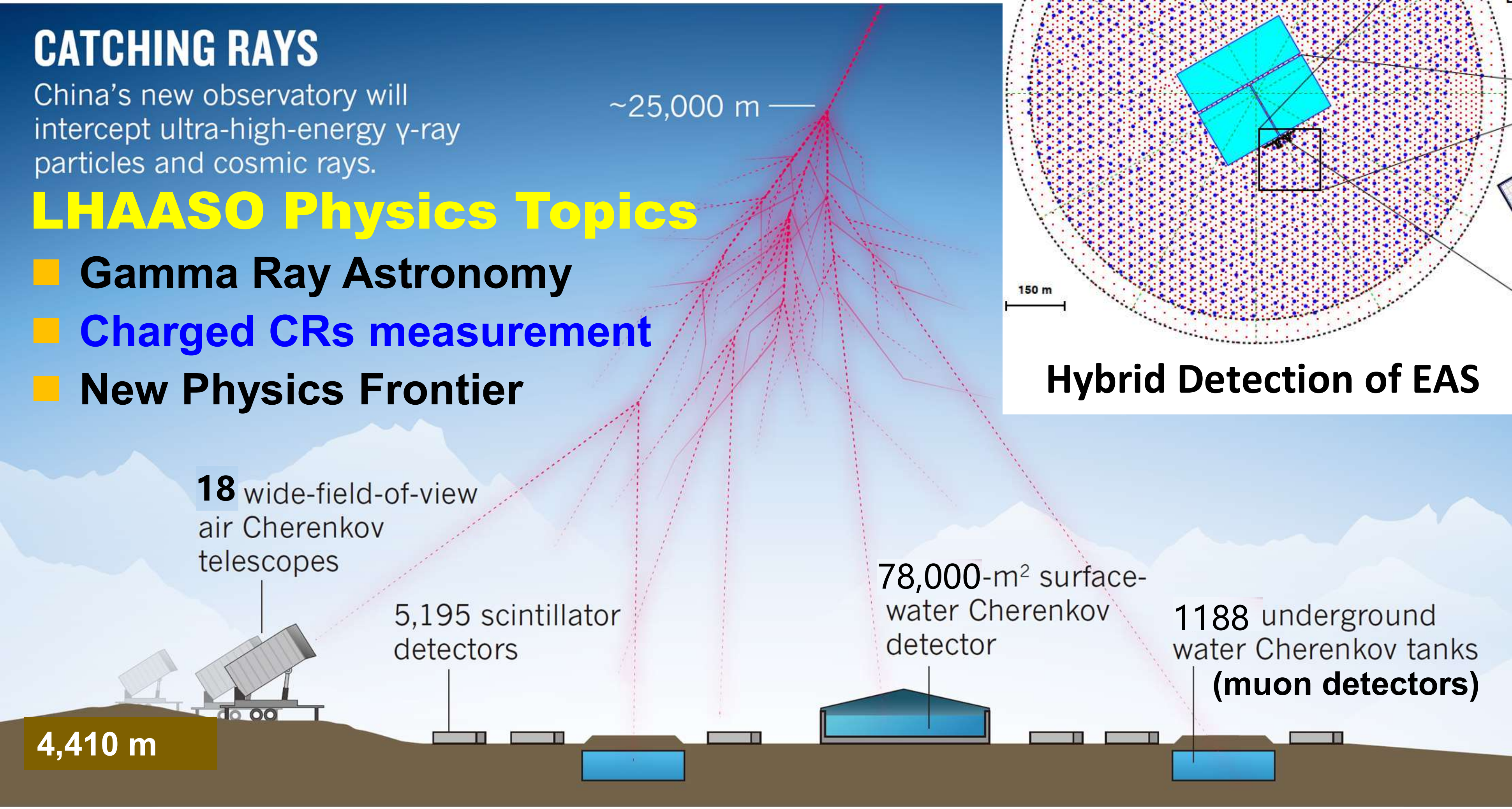

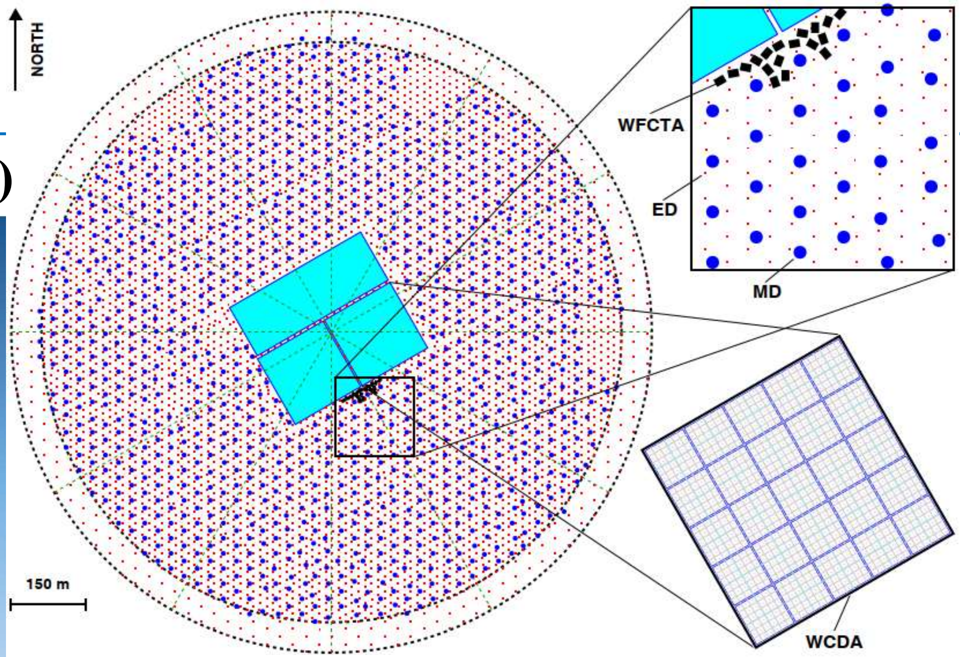

Hybrid Detection of EAS

Table 1. LHAASO vs other EAS arrays

Experiment	depth g/cm^2	Detector	ΔE (eV)	e.m. Sensitive Area (m^2)	Instrumented Area (m^2)	Coverage
ARGO-YBJ	606	RPC/hybrid	$3\times10^{11}-10^{16}$	6700	11,000	0.93 (central carpet)
BASJE-MAS	550	scint./muon	$6\cdot10^{12}-3.5\cdot10^{16}$		10^4	
TIBET ASγ	606	scint./burst det.	$5\times10^{13}-10^{17}$	380	3.7×10^4	10^{-2}
CASA-MIA	860	scint./muon	$10^{14}-3.5\cdot10^{16}$	1.6×10^3	2.3×10^5	7×10^{-3}
KASCADE	1020	scint./mu/had	$10^{15}-10^{17}$	5×10^2	4×10^4	
KASCADE -Grande	1020	scint./mu/had	$10^{16}-10^{18}$	370	5×10^5	7×10^{-4}
Tunka	900	open Cher.det.	$3\cdot10^{15}-3\cdot10^{18}$	-	10^6	-
IceTop	680	ice Cher.det.	$10^{15}-10^{18}$	4.2×10^2	10^6	4×10^{-4}
LHAASO	600	Water C scint./mu/had Wide FoV Cher.Tel	$3\times10^{11}-10^{18}$	5.2×10^3	1.3×10^6	4×10^{-3} [KM2A]

Muon detectors

Experiment	m asl	μ Sensitive Area [m^2]	Instrumented Area [m^2]	Coverage
LHAASO	4410	4.2×10^4	10^6	4.4×10^{-2}
TIBET ASγ	4300	4.5×10^3	3.7×10^4	1.2×10^{-1}
KASCADE	110	6×10^2	4×10^4	1.5×10^{-2}
CASA-MIA	1450	2.5×10^3	2.3×10^5	1.1×10^{-2}

The Site

Bird's eye view of LHAASO， 2021-08

- **Location： 29o21' 27.6" N , 100o08'19.6" E**
- **Altitude: 4410 m**
- **2021-07 completed built and in operation**

LHAASO, *Nature Astronomy 5:849 (2021)*

(Aug. 2018, at 4410 m a.s.l.)

LHAASO: Multi-Messenger Collaboration Network

The LHAASO collaboration has signed MOUs with 8 international detector collaboration.

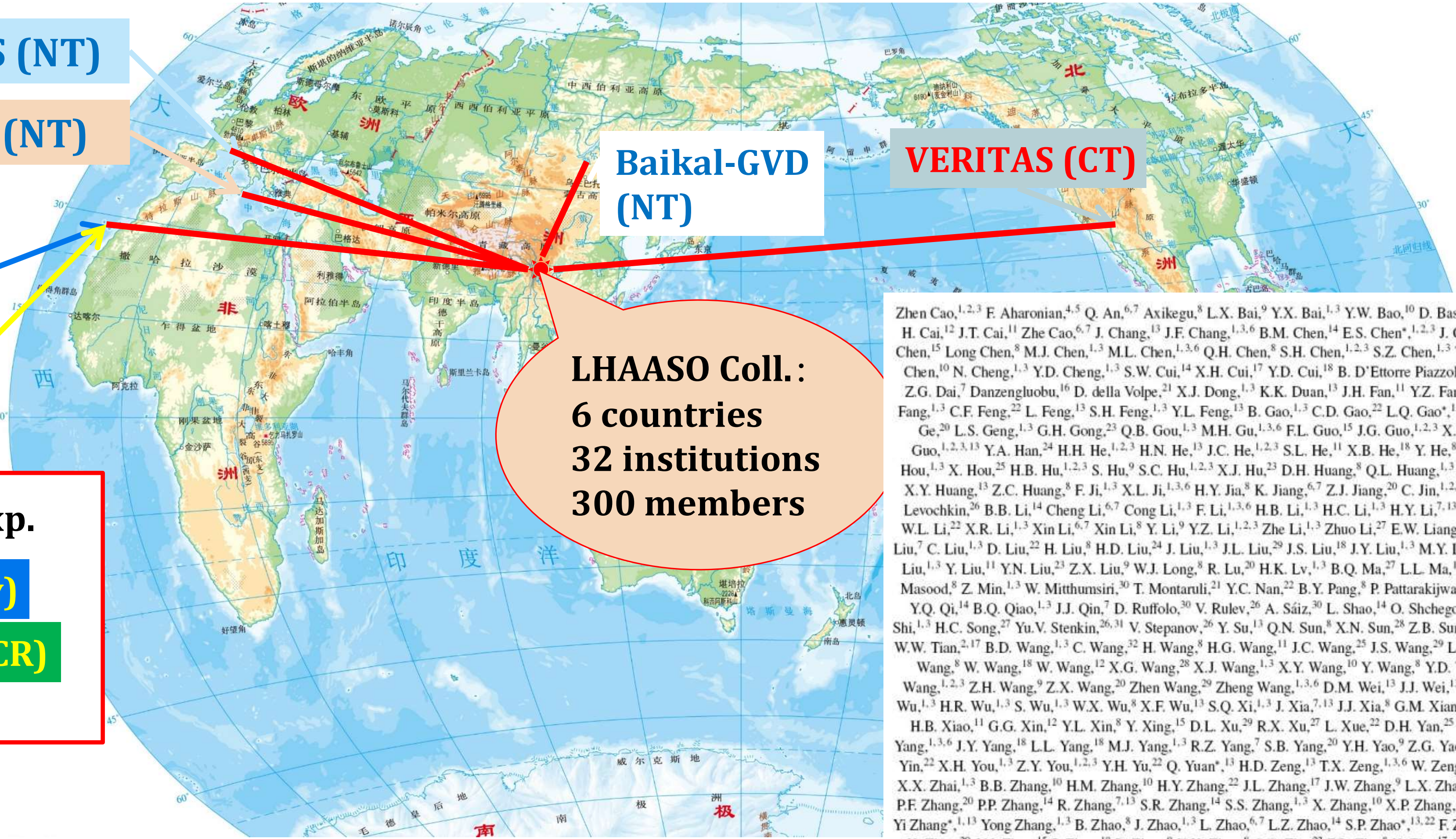

Zhen Cao,[1,2,3] F. Aharonian,[4,5] Q. An,[6,7] Axikegu,[8] L.X. Bai,[9] Y.X. Bai,[1,3] Y.W. Bao,[10] D. Bastieri,[11] X.J. Bi*,[1,2,3] Y.J. Bi,[1,3] H. Cai,[12] J.T. Cai,[11] Zhe Cao,[6,7] J. Chang,[13] J.F. Chang,[1,3,6] B.M. Chen,[14] E.S. Chen*,[1,2,3] J. Chen,[9] Liang Chen,[1,2,3] Liang Chen,[15] Long Chen,[8] M.J. Chen,[1,3] M.L. Chen,[1,3,6] Q.H. Chen,[8] S.H. Chen,[1,2,3] S.Z. Chen,[1,3] T.L. Chen,[16] X.L. Chen,[1,2,3] Y. Chen,[10] N. Cheng,[1,3] Y.D. Cheng,[1,3] S.W. Cui,[14] X.H. Cui,[17] Y.D. Cui,[18] B. D'Ettorre Piazzoli,[19] B.Z. Dai,[20] H.L. Dai,[1,3,6] Z.G. Dai,[7] Danzengluobu,[16] D. della Volpe,[21] X.J. Dong,[1,3] K.K. Duan,[13] J.H. Fan,[11] Y.Z. Fan,[13] Z.X. Fan,[1,3] J. Fang,[20] K. Fang,[1,3] C.F. Feng,[22] L. Feng,[13] S.H. Feng,[1,3] Y.L. Feng,[13] B. Gao,[1,3] C.D. Gao,[22] L.Q. Gao*,[1,2,3] Q. Gao,[16] W. Gao,[22] M.M. Ge,[20] L.S. Geng,[1,3] G.H. Gong,[23] Q.B. Gou,[1,3] M.H. Gu,[1,3,6] F.L. Guo,[15] J.G. Guo,[1,2,3] X.L. Guo,[8] Y.Q. Guo,[1,3] Y.Y. Guo,[1,2,3,13] Y.A. Han,[24] H.H. He,[1,2,3] H.N. He,[13] J.C. He,[1,2,3] S.L. He,[11] X.B. He,[18] Y. He,[8] M. Heller,[21] Y.K. Hor,[18] C. Hou,[1,3] X. Hou,[25] H.B. Hu,[1,2,3] S. Hu,[9] S.C. Hu,[1,2,3] X.J. Hu,[23] D.H. Huang,[8] Q.L. Huang,[1,3] W.H. Huang,[22] X.T. Huang,[22] X.Y. Huang,[13] Z.C. Huang,[8] F. Ji,[1,3] X.L. Ji,[1,3,6] H.Y. Jia,[8] K. Jiang,[6,7] Z.J. Jiang,[20] C. Jin,[1,2,3] T. Ke,[1,3] D. Kuleshov,[26] K. Levochkin,[26] B.B. Li,[14] Cheng Li,[6,7] Cong Li,[1,3] F. Li,[1,3,6] H.B. Li,[1,3] H.C. Li,[1,3] H.Y. Li,[7,13] Jian Li,[7] Jie Li,[1,3,6] K. Li,[1,3] W.L. Li,[22] X.R. Li,[1,3] Xin Li,[6,7] Xin Li,[8] Y. Li,[9] Y.Z. Li,[1,2,3] Zhe Li,[1,3] Zhuo Li,[27] E.W. Liang,[28] Y.F. Liang,[28] S.J. Lin,[18] B. Liu,[7] C. Liu,[1,3] D. Liu,[22] H. Liu,[8] H.D. Liu,[24] J. Liu,[1,3] J.L. Liu,[29] J.S. Liu,[18] J.Y. Liu,[1,3] M.Y. Liu,[16] R.Y. Liu,[10] S.M. Liu,[8] W. Liu,[1,3] Y. Liu,[11] Y.N. Liu,[23] Z.X. Liu,[9] W.J. Long,[8] R. Lu,[20] H.K. Lv,[1,3] B.Q. Ma,[27] L.L. Ma,[1,3] X.H. Ma,[1,3] J.R. Mao,[25] A. Masood,[8] Z. Min,[1,3] W. Mitthumsiri,[30] T. Montaruli,[21] Y.C. Nan,[22] B.Y. Pang,[8] P. Pattarakijwanich,[30] Z.Y. Pei,[11] M.Y. Qi,[1,3] Y.Q. Qi,[14] B.Q. Qiao,[1,3] J.J. Qin,[7] D. Ruffolo,[30] V. Rulev,[26] A. Sáiz,[30] L. Shao,[14] O. Shchegolev,[26,31] X.D. Sheng,[1,3] J.R. Shi,[1,3] H.C. Song,[27] Yu.V. Stenkin,[26,31] V. Stepanov,[26] Y. Su,[13] Q.N. Sun,[8] X.N. Sun,[28] Z.B. Sun,[32] P.H.T. Tam,[18] Z.B. Tang,[6,7] W.W. Tian,[2,17] B.D. Wang,[1,3] C. Wang,[32] H. Wang,[8] H.G. Wang,[11] J.C. Wang,[25] J.S. Wang,[29] L.P. Wang,[22] L.Y. Wang,[1,3] R.N. Wang,[8] W. Wang,[18] W. Wang,[12] X.G. Wang,[28] X.J. Wang,[1,3] X.Y. Wang,[10] Y. Wang,[8] Y.D. Wang,[1,3] Y.J. Wang,[1,3] Y.P. Wang,[1,2,3] Z.H. Wang,[9] Z.X. Wang,[20] Zhen Wang,[29] Zheng Wang,[1,3,6] D.M. Wei,[13] J.J. Wei,[13] Y.J. Wei,[1,2,3] T. Wen,[20] C.Y. Wu,[1,3] H.R. Wu,[1,3] S. Wu,[1,3] W.X. Wu,[8] X.F. Wu,[13] S.Q. Xi,[1,3] J. Xia,[7,13] J.J. Xia,[8] G.M. Xiang,[2,15] D.X. Xiao,[16] G. Xiao,[1,3] H.B. Xiao,[11] G.G. Xin,[12] Y.L. Xin,[8] Y. Xing,[15] D.L. Xu,[29] R.X. Xu,[27] L. Xue,[22] D.H. Yan,[25] J.Z. Yan,[13] C.W. Yang,[9] F.F. Yang,[1,3,6] J.Y. Yang,[18] L.L. Yang,[18] M.J. Yang,[1,3] R.Z. Yang,[7] S.B. Yang,[20] Y.H. Yao,[9] Z.G. Yao,[1,3] Y.M. Ye,[23] L.Q. Yin,[1,3] N. Yin,[22] X.H. You,[1,3] Z.Y. You,[1,2,3] Y.H. Yu,[22] Q. Yuan*,[13] H.D. Zeng,[13] T.X. Zeng,[1,3,6] W. Zeng,[20] Z.K. Zeng,[1,2,3] M. Zha,[1,3] X.X. Zhai,[1,3] B.B. Zhang,[10] H.M. Zhang,[10] H.Y. Zhang,[22] J.L. Zhang,[17] J.W. Zhang,[9] L.X. Zhang,[11] Li Zhang,[20] Lu Zhang,[14] P.F. Zhang,[20] P.P. Zhang,[14] R. Zhang,[7,13] S.R. Zhang,[14] S.S. Zhang,[1,3] X. Zhang,[10] X.P. Zhang,[1,3] Y.F. Zhang,[8] Y.L. Zhang,[1,3] Yi Zhang*,[1,13] Yong Zhang,[1,3] B. Zhao,[8] J. Zhao,[1,3] L. Zhao,[6,7] L.Z. Zhao,[14] S.P. Zhao*,[13,22] F. Zheng,[32] Y. Zheng,[8] B. Zhou,[1,3] H. Zhou,[29] J.N. Zhou,[15] P. Zhou,[10] R. Zhou,[9] X.X. Zhou,[8] C.G. Zhu,[22] F.R. Zhu,[8] H. Zhu,[17] K.J. Zhu,[1,2,3,6] and X. Zuo[1,3]

Operation of LHAASO

- KM2A is operated with >99.4% duty cycle and event rate 2x10⁸ /day
- WCDA is operated with 98.4% and event rate 3x10⁹ /day
- Data acquisition time of WFCTA >1400 hrs and number of matched events ~70 million

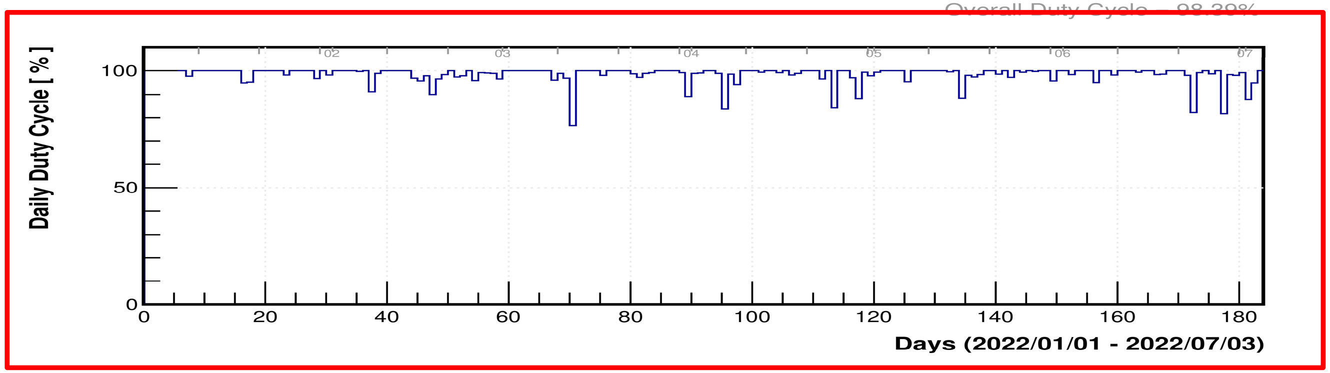

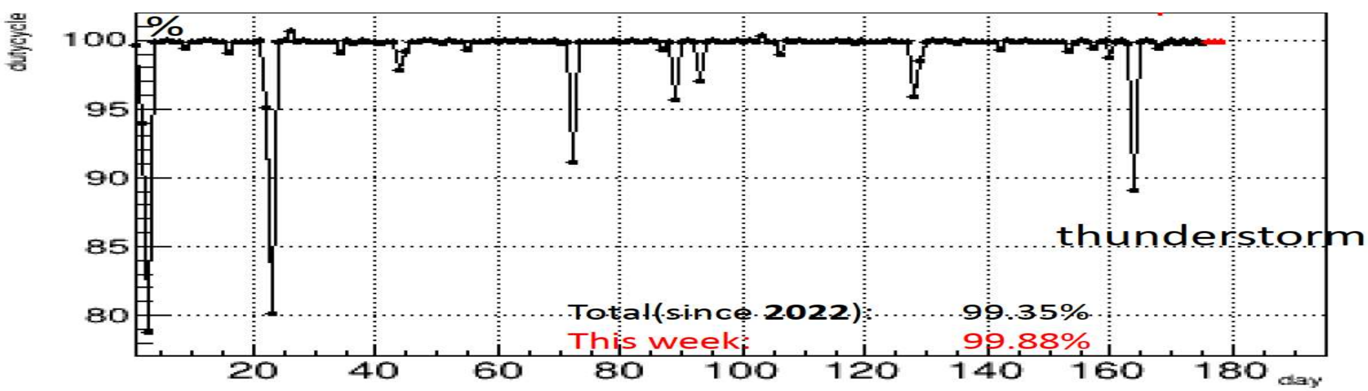

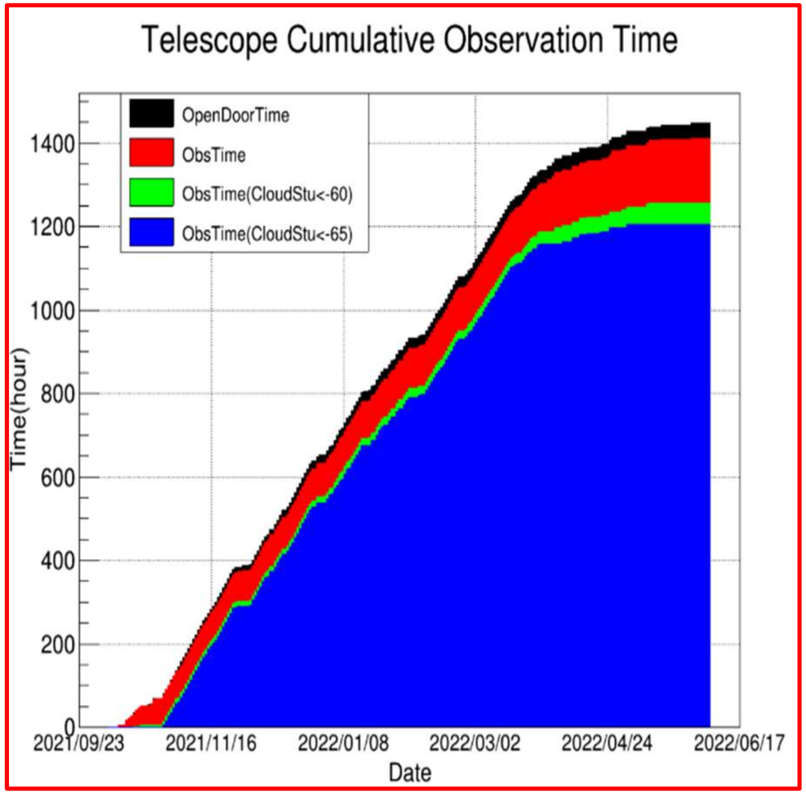

◻ CR Spectra around the Knees

- Pure Protons
- Light Component (H + He)
- All Particle Spectrum and Composition

Hybrid Measurement of CR Showers around the Knee

- **WFCTA: Cherenkov telescopes**
  1. Number of pixels: Npix≥7
  2. FoV: 10° × 10° out of 16° × 16° for the centroid of the image
  3. R_p: 150 – 300 m

- **KM2A:**
  1. Core (x,y)
     - $\sqrt{x^2+y^2} < 470\ m$
     - !|x'|<200m & !|x'|<160m
  2. Number of fired EDs > 20

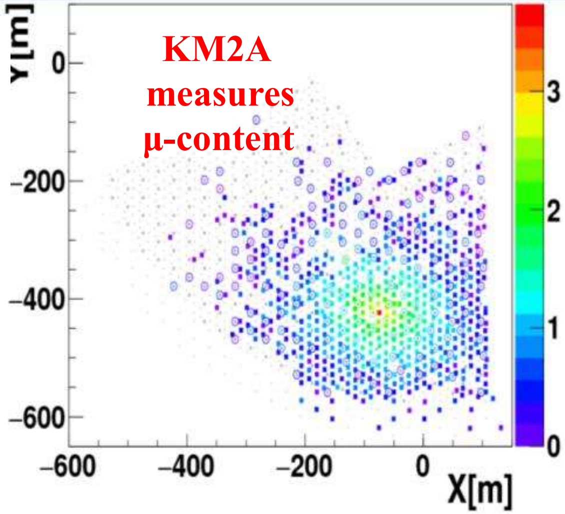

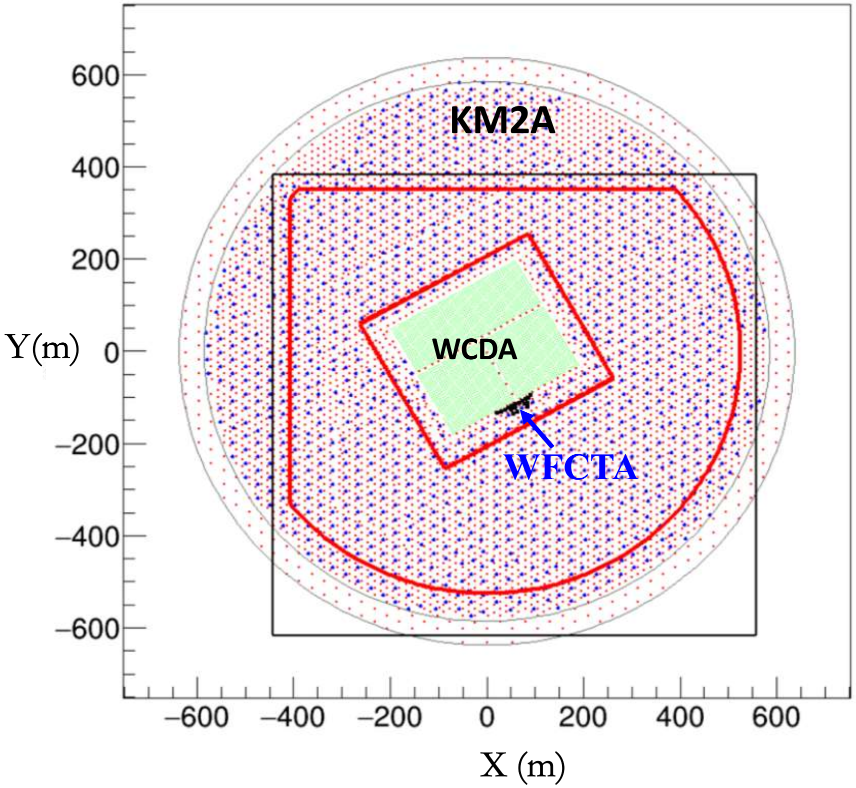

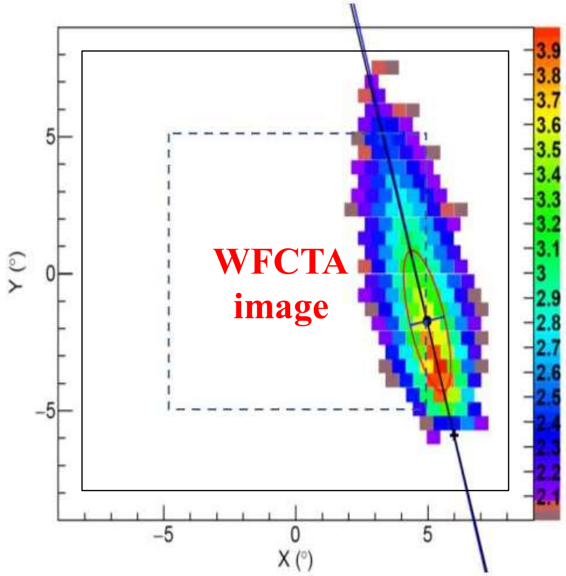

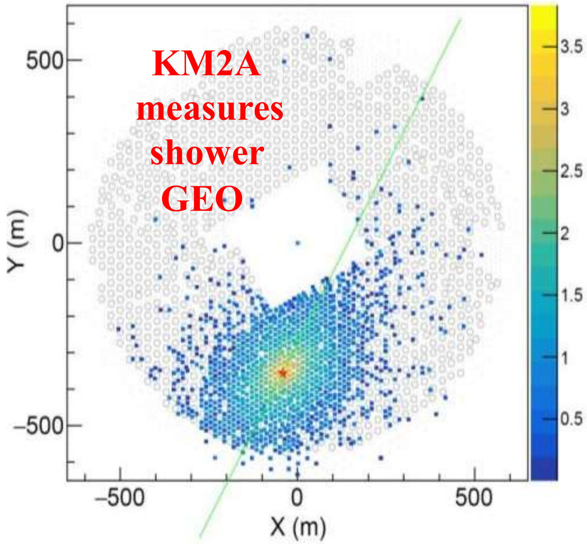

Xmax Measurement by WFCTA

EAS maximum at X_{max} : $X_{max}^{A} = X_{max}^{P} - \lambda_r \ln A$

Elongation rate : $\Lambda \equiv \frac{dX_{max}}{d\log_{10}E} \approx 58\mathrm{g} \cdot \mathrm{cm}^{-2}/\mathrm{decade}$

- $P_0 = \theta_c / \cos zenith - 1.32 \times 10^{-2} R_p$
- $P_X = P_0 + 0.13 \times \lg^2 E_{rec} - 2.16 \times \lg E_{rec}$

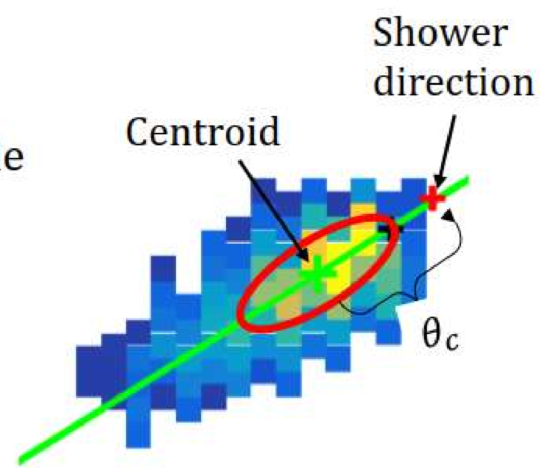

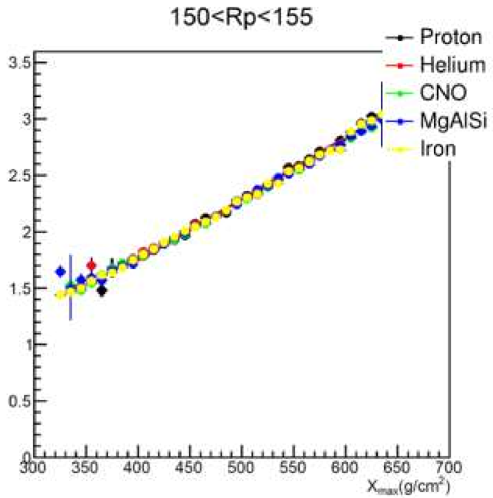

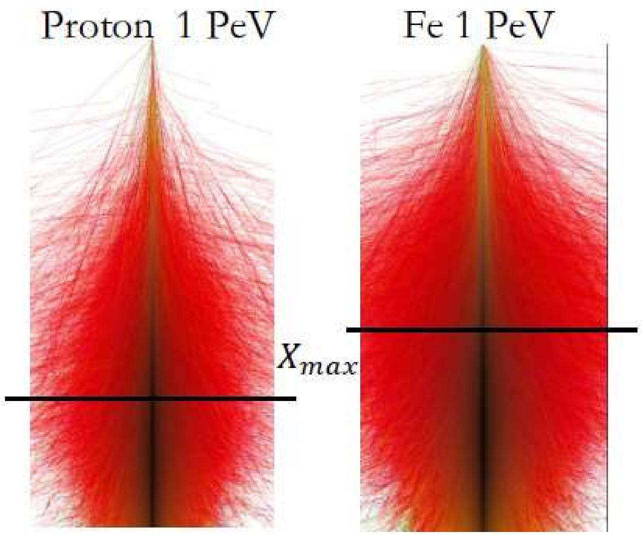

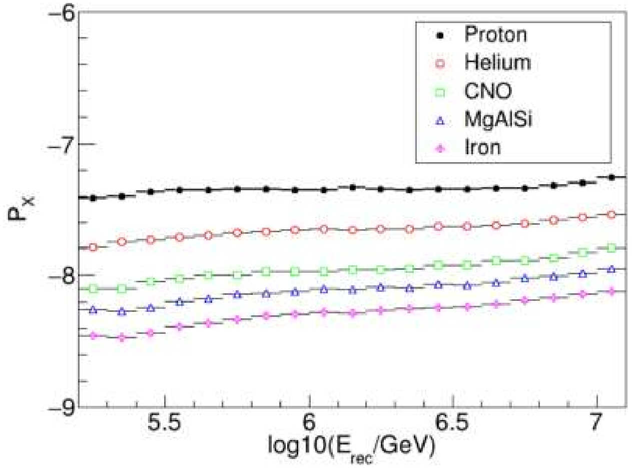

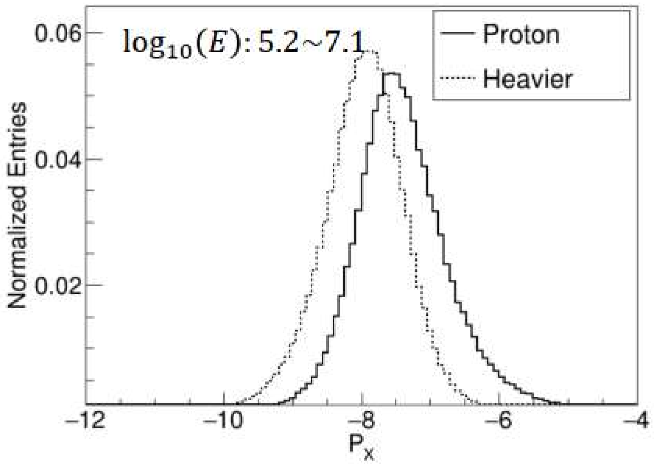

Muon Content in Showers

$$P_{\mu e} = \log_{10} \frac{\rho_\mu}{\rho_e^{0.83}}$$

ρ_μ: *muon density in the ring between* 40*m and* 200*m* from the core

ρ_e: *EM − particle density in the ring between* 40*m and* 200*m*

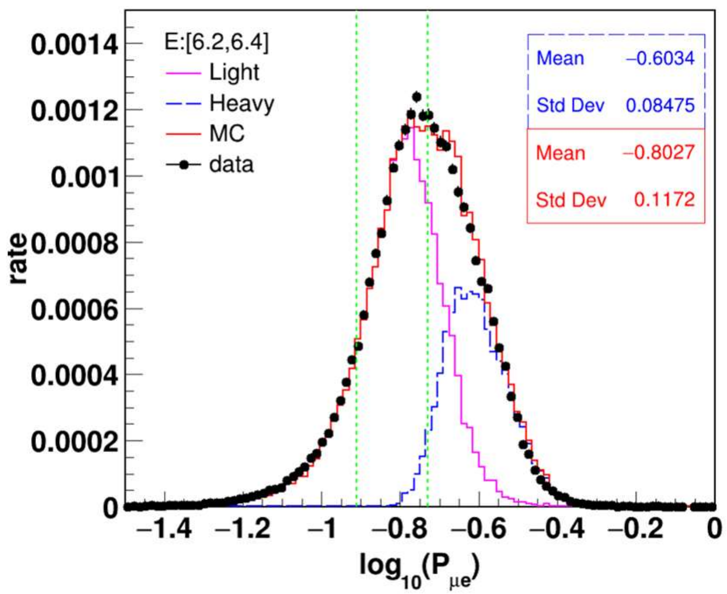

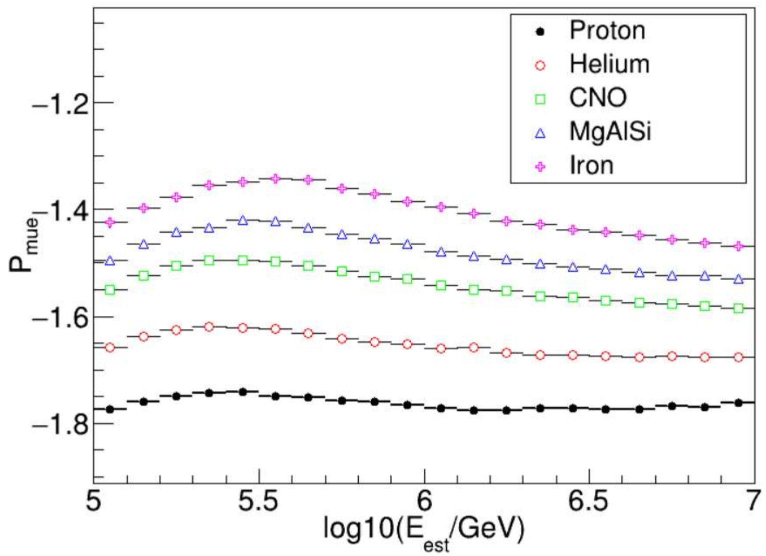

Proton Shower Selection:
shower maximum depth & μ-content

Proton Purity： $\epsilon^{p} = \frac{N_{sel}^{P}}{N_{sel}^{MC}} > 90\%$

$(for\ Eproton > 300\text{TeV})$

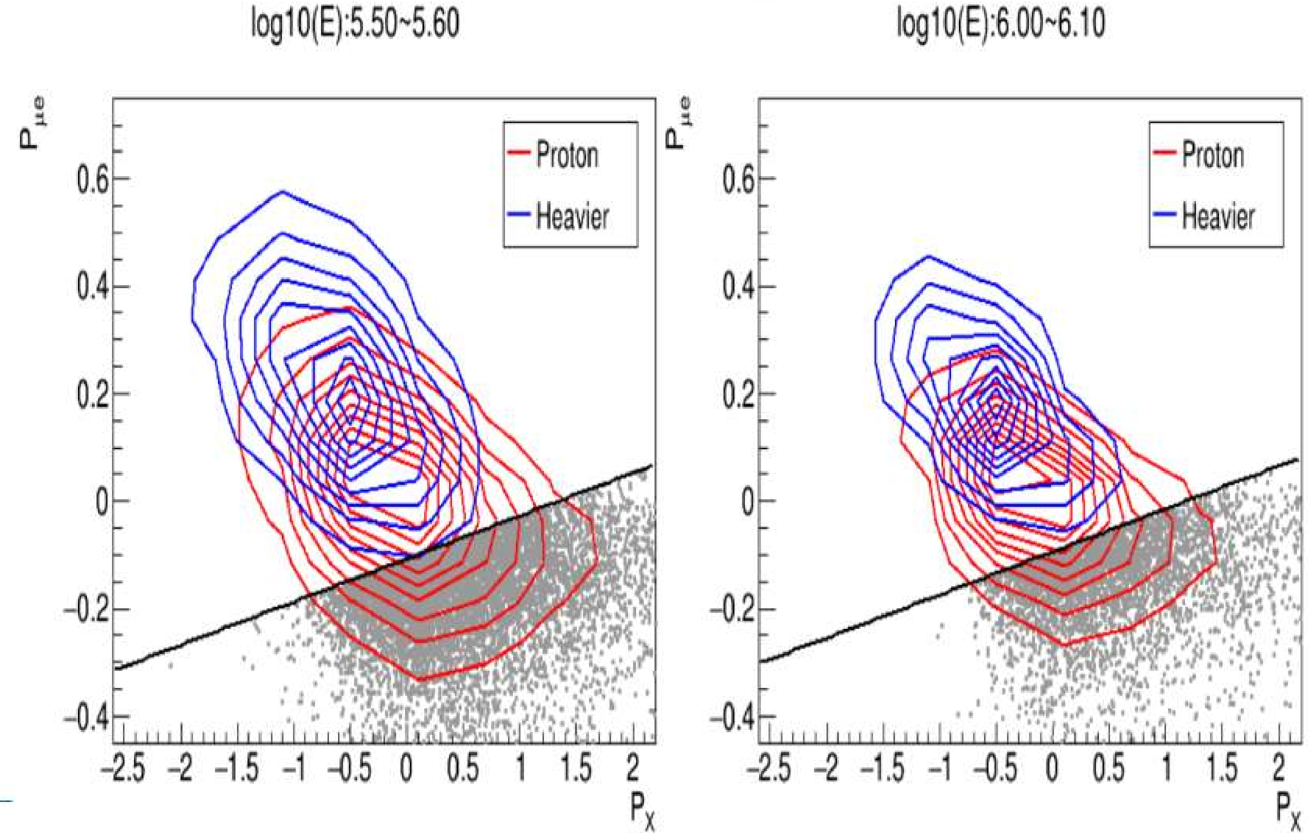

Composition： $\epsilon^{i} = \frac{N_{sel}^{i}}{\Sigma N_{sel}^{i}}$ i= H, He, Other

(After selection)

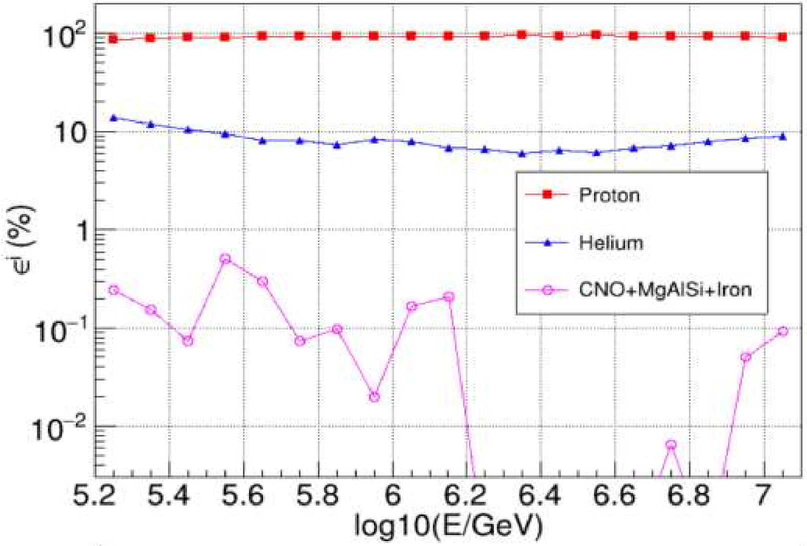

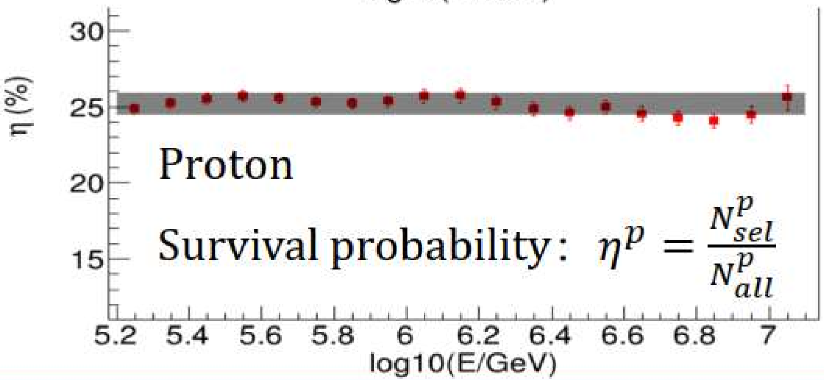

Proton Energy Reconstruction

高海拔宇宙线观测站 Large High Altitude Air Shower Observatory

- **Energy Resolution：<15%**
- **Systematic Bias：<2%**
  (independent of shower energy)
- **Uncertainty mainly due to hadronic interaction models：~1.4%**

$$N_{c\mu} = N_{ph} + CN_{u}$$
$$E_{rec} = kN_{c\mu}$$

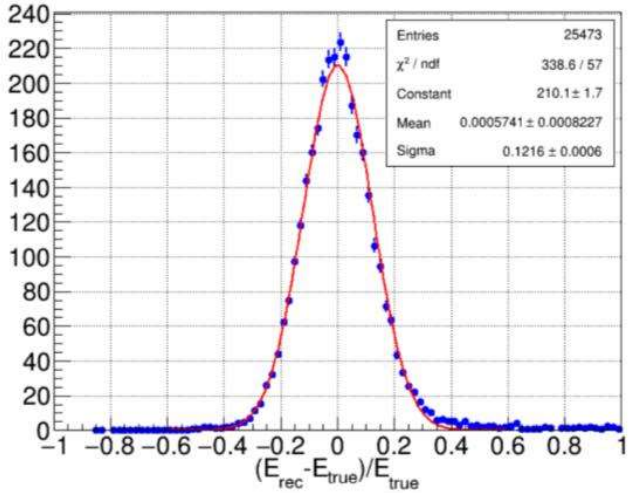

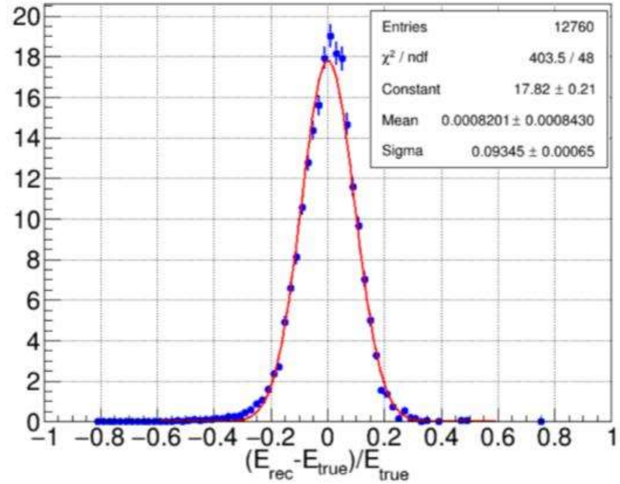

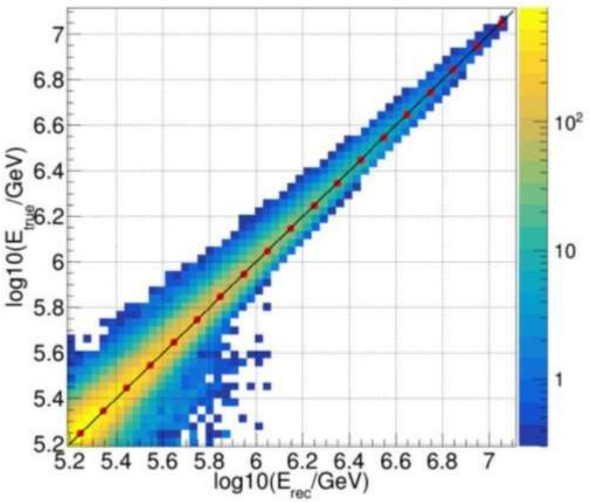

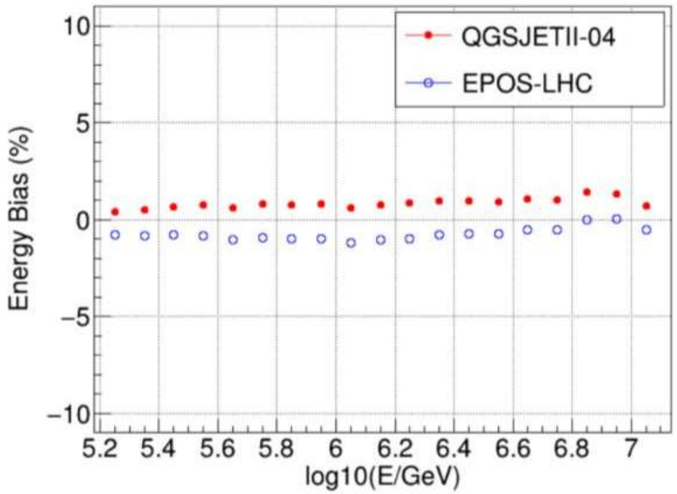

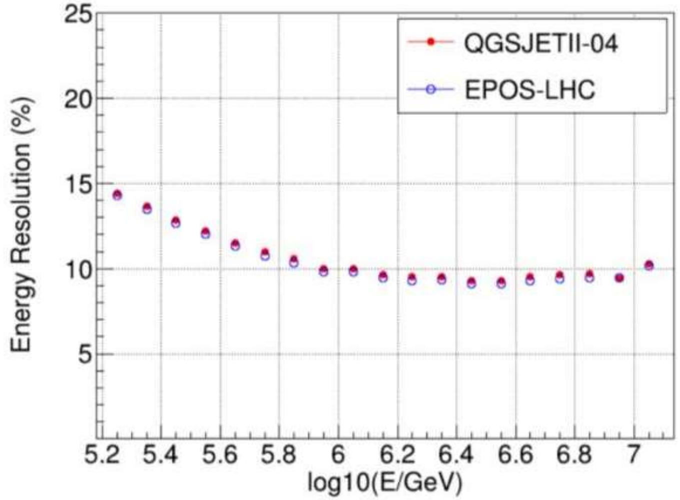

Tests using generated samples

Ratio of proton vs Helium nuclei in composition assumptions

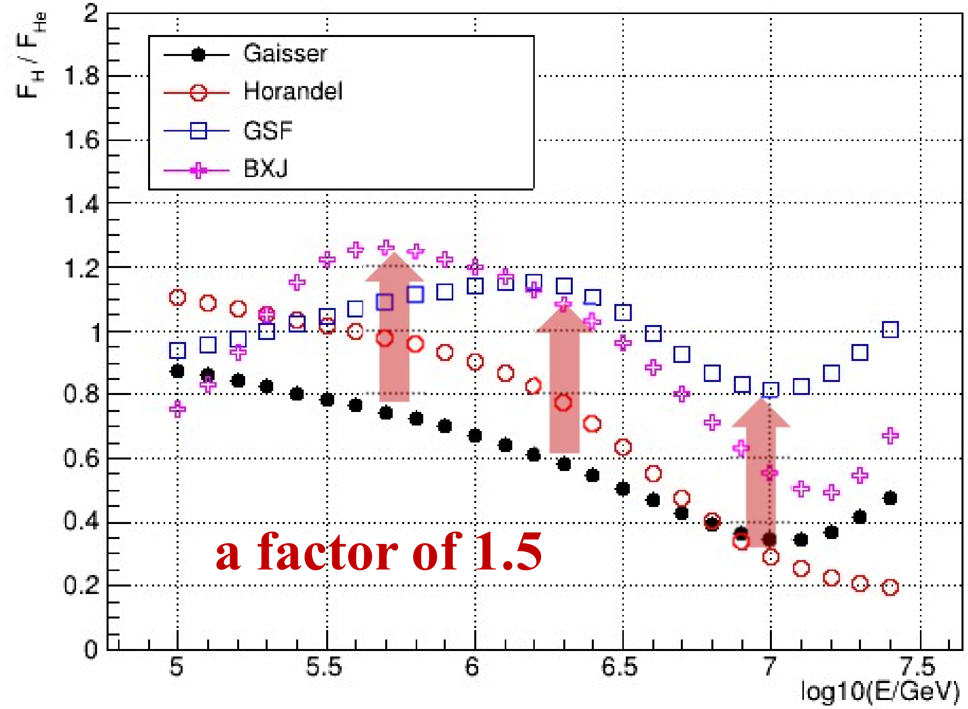

Re-produced pure-proton spectra under 4 assumption of composition mixtures

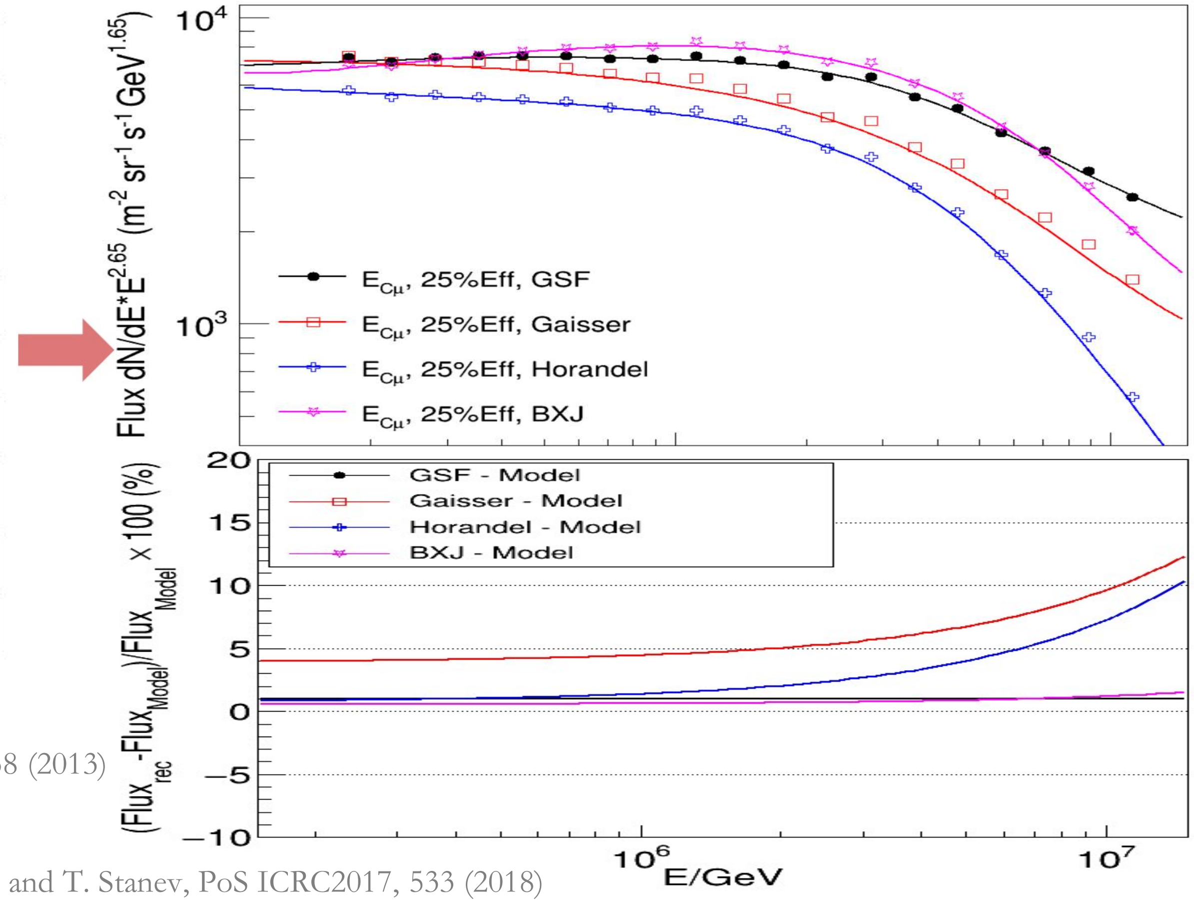

Gaisser Model: Gaisser, T.K., Stanev, T. & Tilav, S. Front. Phys. 8, 748 – 758 (2013)

Horandel Model: Horandel J R. Astroparticle Physics, 2003, 19(2):193 – 220

GSF Model: H. P. Dembinski, R. Engel, A. Fedynitch, T. Gaisser, F. Riehn, and T. Stanev, PoS ICRC2017, 533 (2018)

BXJ Model: Lv X.-J., Bi X.-J., Fang K., et al. , arXiv:2403.11832. (2024)

Light component (H+He) events selection

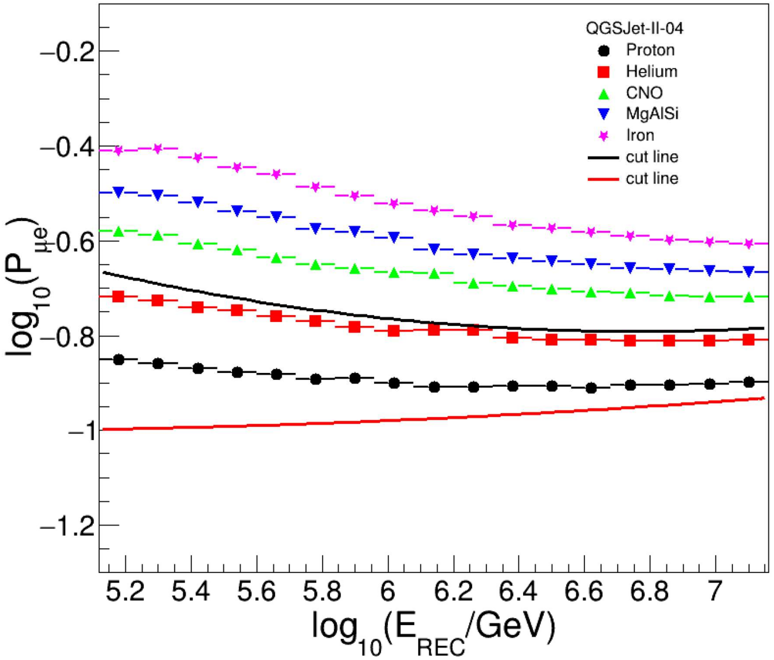

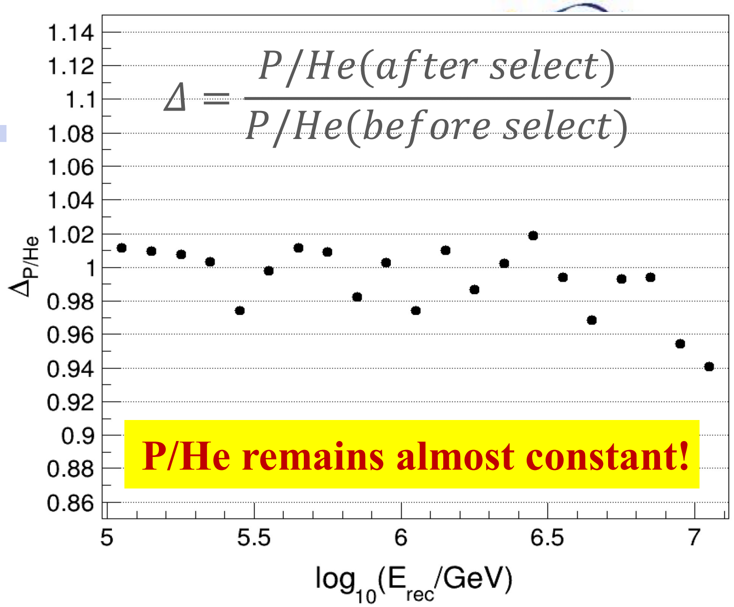

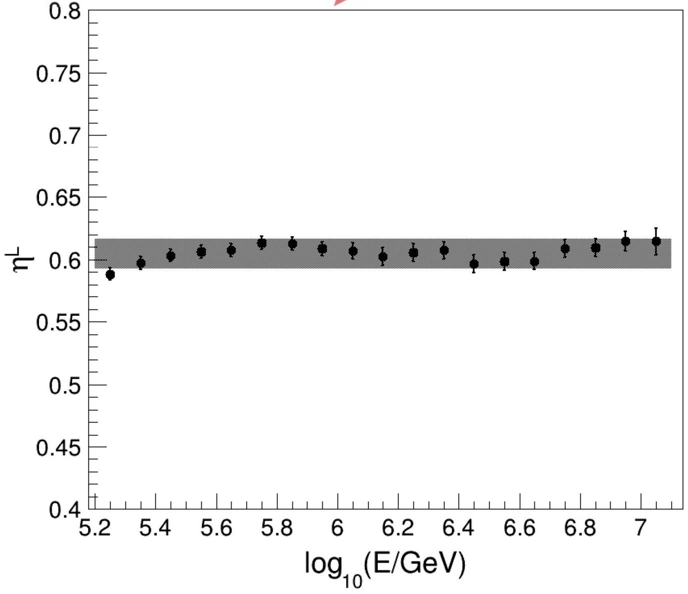

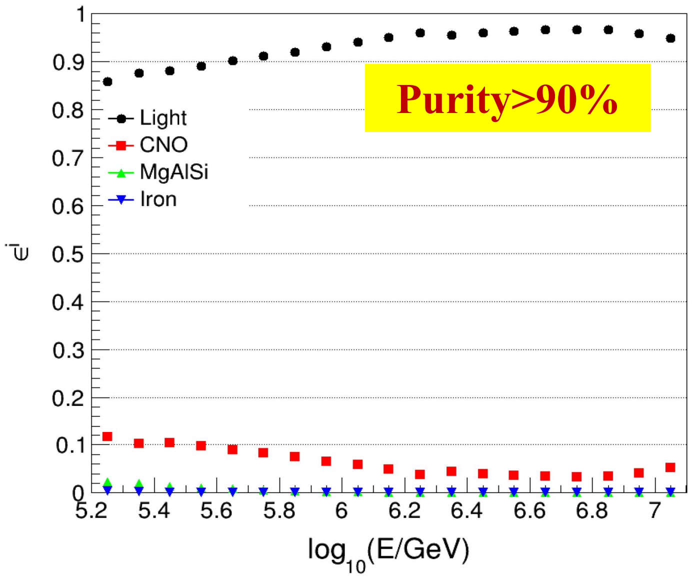

$$\eta^l = \frac{N^L_{select}}{N^L_{all}}$$

$$\epsilon^l = \frac{N^L_{select}}{N^L_{select}+N^H_{select}}$$

Light component (H+He) → Helium Spectrum

Different composition models test

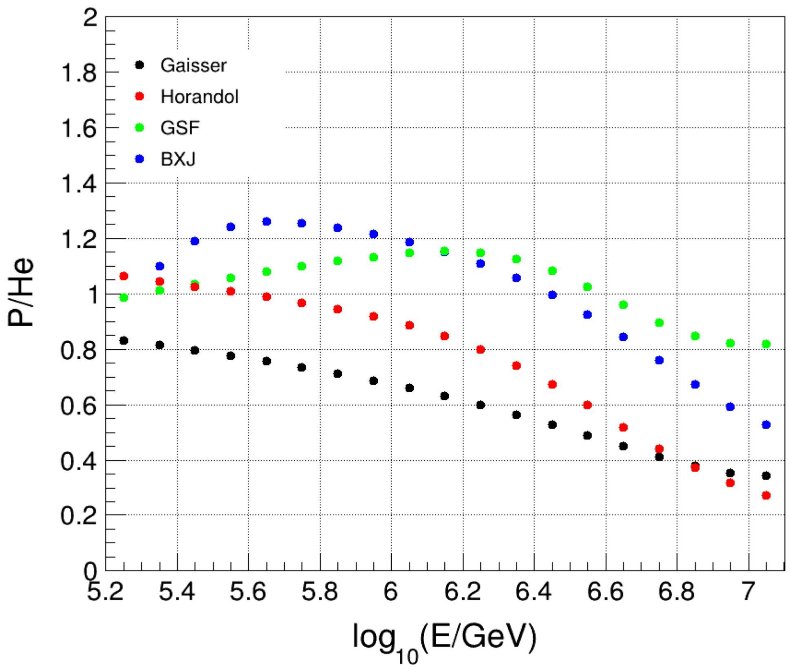

After dual cuts

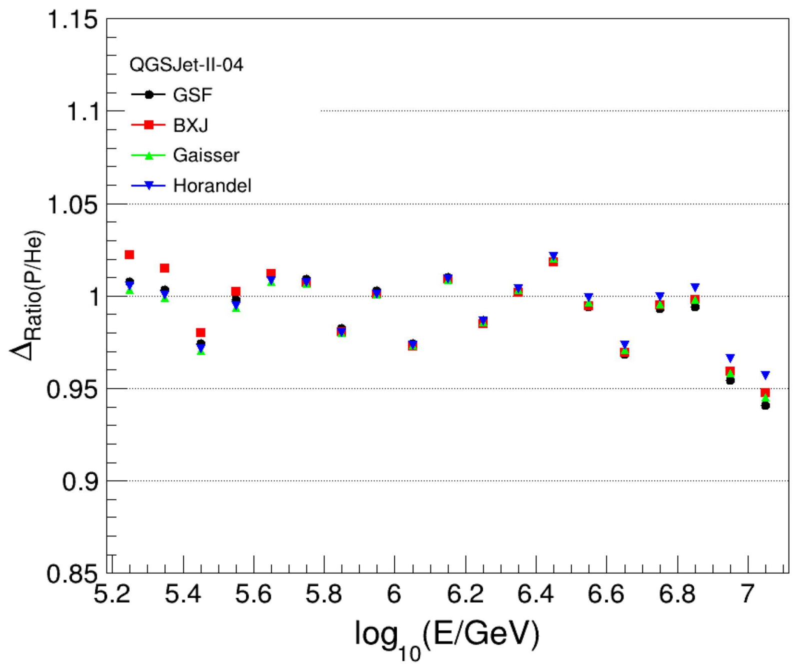

- **The P to He ratio after composition selection is almost the same as before**
  - **The variation of the P/He ratio is within ±3% after composition selection**
- **Light component (H+He) Spectrum – Proton Spectrum → Helium Spectrum**

All-particle energy spectrum & composition by LHAASO

(from 0.3 to 30 PeV)

LHAASO Collaboration, PHYSICAL REVIEW LETTERS 132, 131002 (2024)

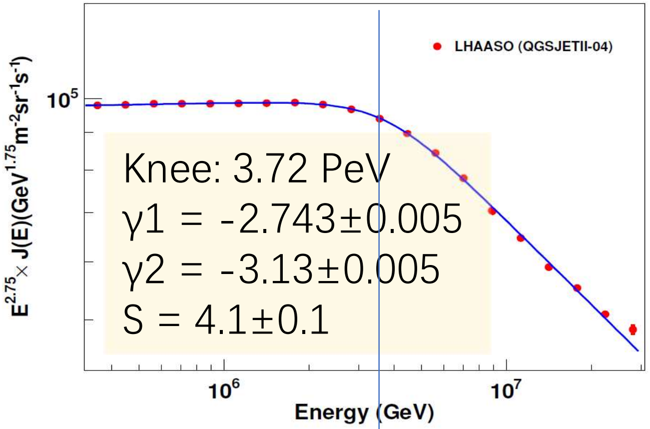

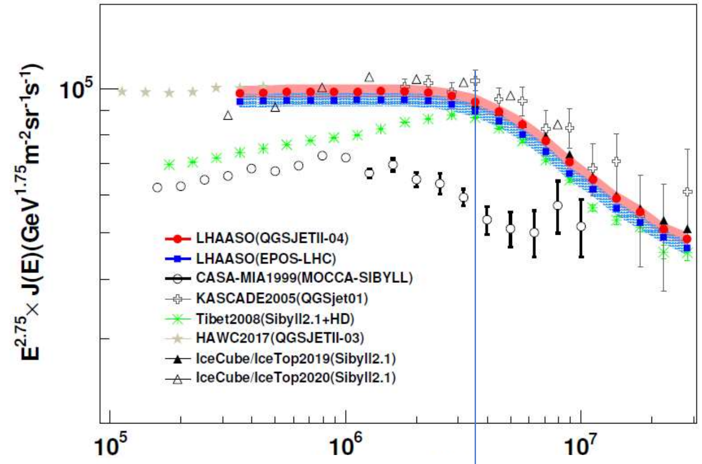

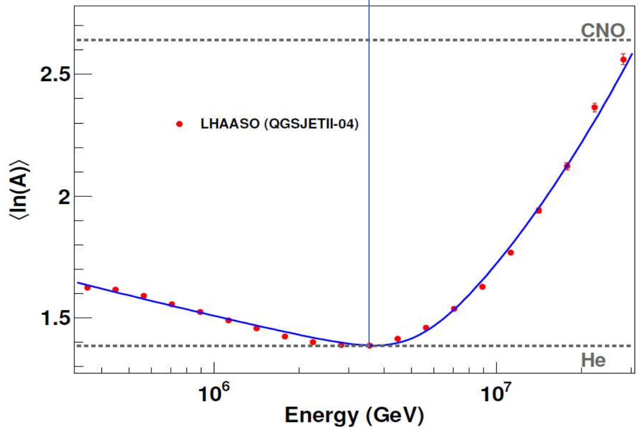

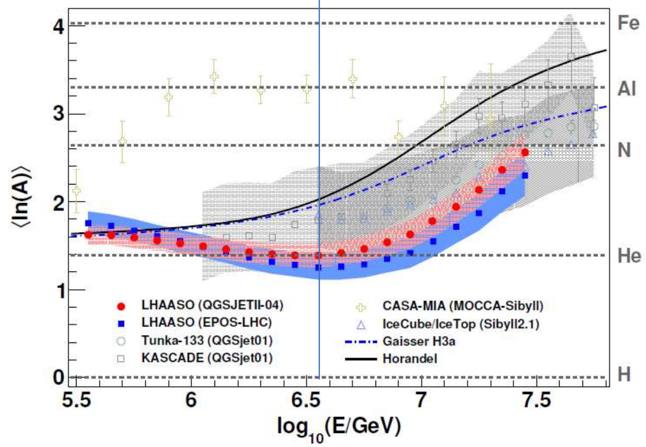

- Systematic uncertainties are sufficiently small
- This unveils a clear correlation between the flux and the composition at the knee

Energy reconstruction

- Energy reconstruction independent of the primary CR component
- Scintillator detector array（ED）： Electromagnetic component （N_e）
- Muon detector array （MD）： *hadron component* $\pi^{\pm} \rightarrow \mu$ （N_{μ}）

$E_0 = E_e + E_h \approx N_e^{max} \times E_c^e + aN_{\mu} \times E_c^{\pi}$ $\quad N_{e\mu} = N_e + aN_{\mu}$ $\quad E_{rec} = b \times N_{e\mu}$

J. Matthews, Astropart. Phys. 22, 387 (2005)

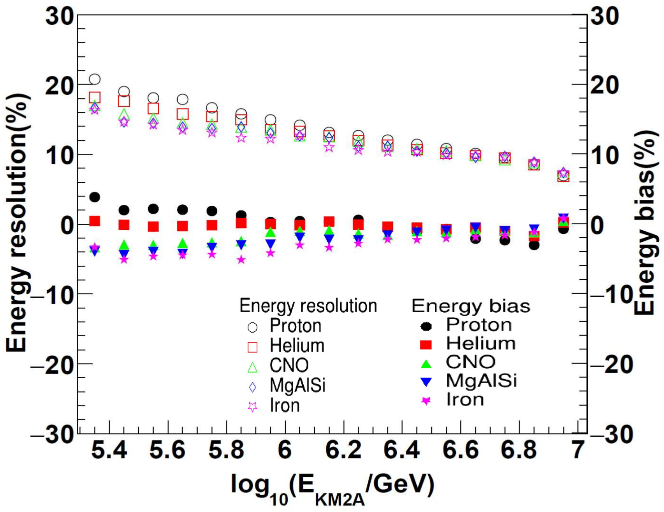

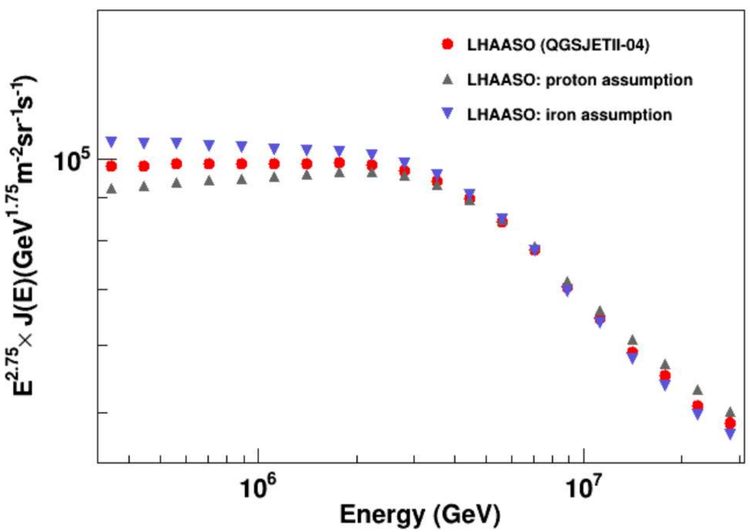

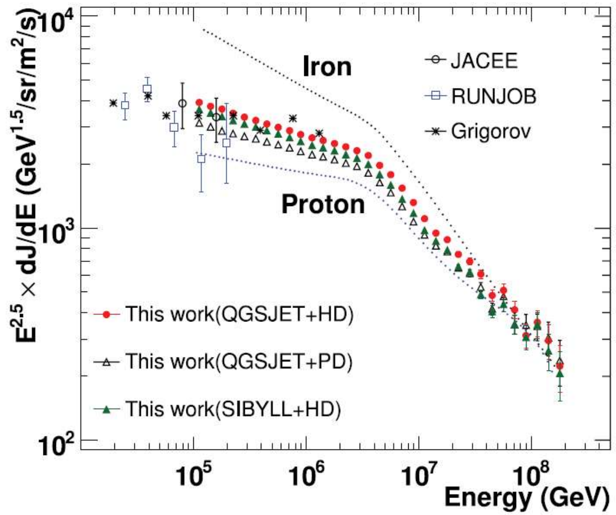

PHYSICAL REVIEW D 106, 123028 (2022)

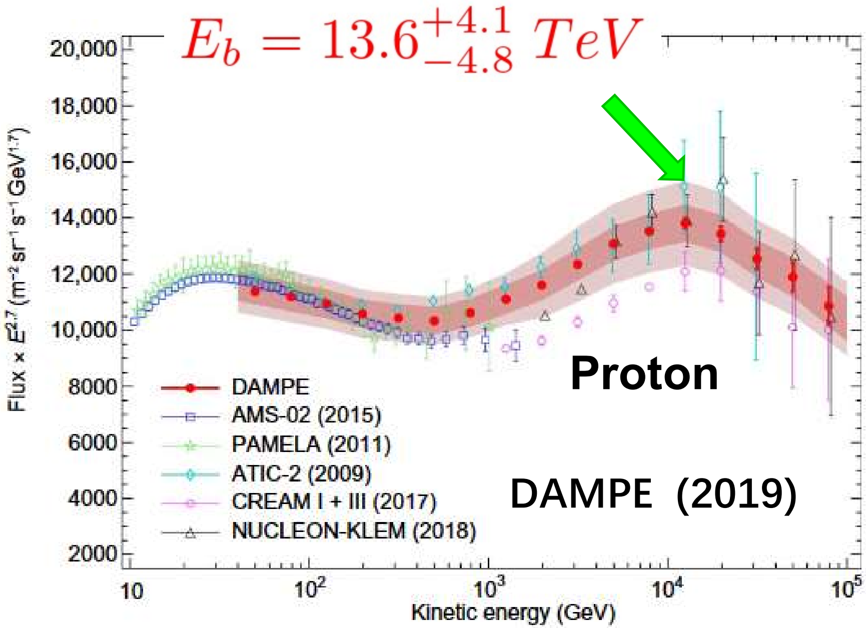

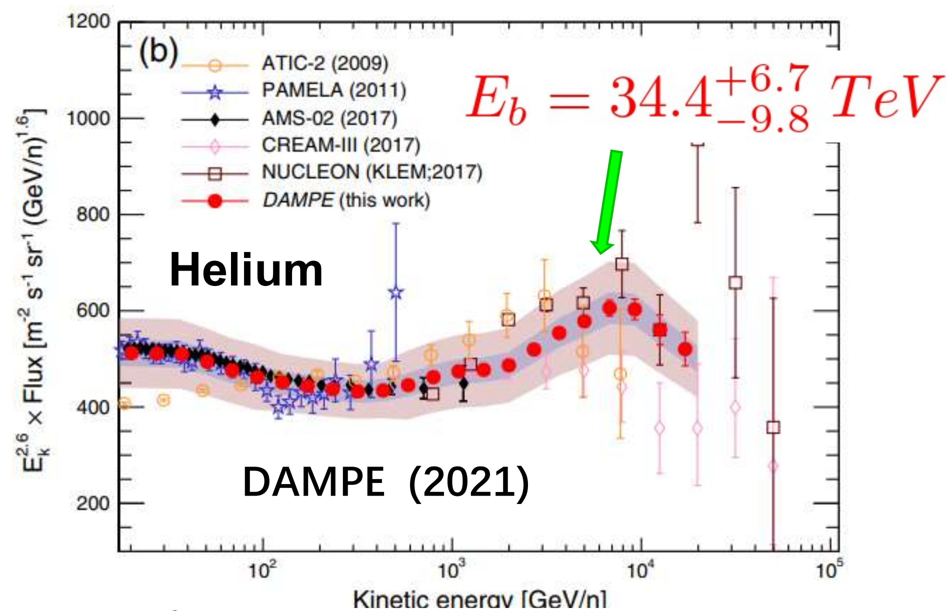

- **Bump: ~13.6 TeV for Proton and**
  ~34.4 TeV for Helium
- **Charge Z dependent?**
  - **The ratio of Proton bump and Helium bump is 2.5 ± 0.8**
- **Iron spectra from 100 TeV to several PeVs will be measured by LHAASO and can answer the question clearly.**

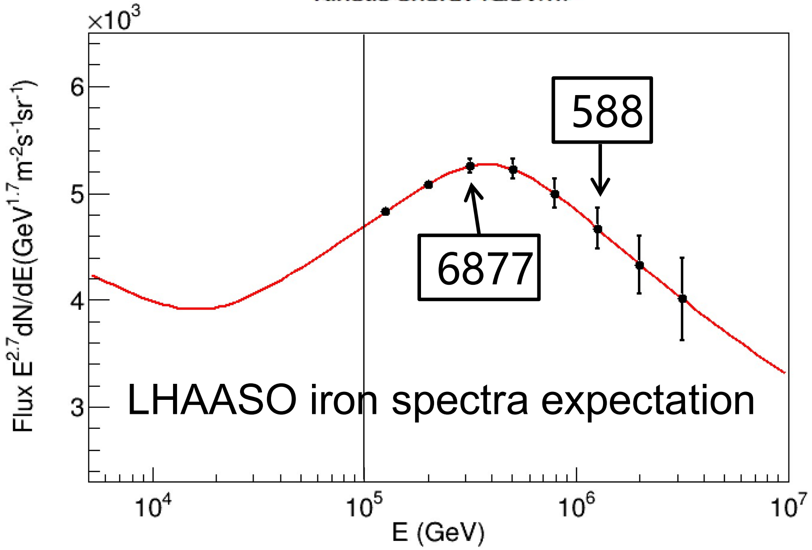

Summary & Outlook

- **Measuring CR Spectra of Individual Species around knees is a big step towards understanding the knee feature**
  - **The spectra of proton, helium and proton+helium around knees are planned to be submitted to the journal this year**
- **All particles energy spectrum from 300 TeV to 30 PeV has been measured by LHAASO-KM2A with high accuracy, revealing a clear correlation between the flux and the composition at the knee**
- **The iron spectrum around 400 TeV will be finished next year**
- **And iron spectrum around the knee is the goal in 3 years.**

Thanks！

LHAASO a complex for both γ-astronomy and Cosmic Ray research

The ½ array started operation in 2019 and the full array in 2021

KM2A: Scintillator counters (ED) and muon counters (MD)

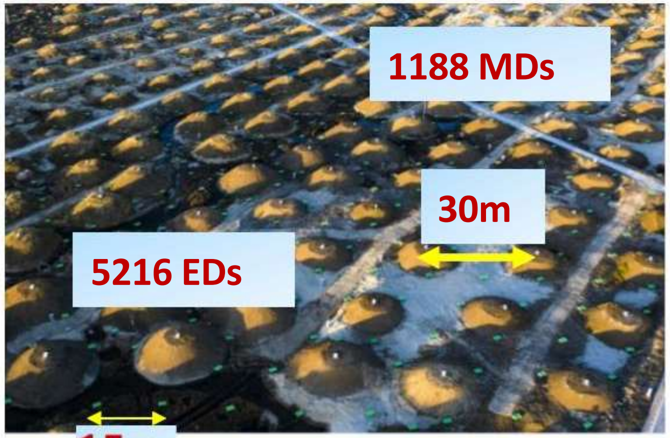

Very sensitive γ-ray telescope above 10 TeV (~15 mCU)

Water Cherenkov Detector Array (78,000 m²)

Very sensitive γ-ray survey telescope above 1 TeV (15 mCU)

Wide FoV Cherenkov Telescope Array

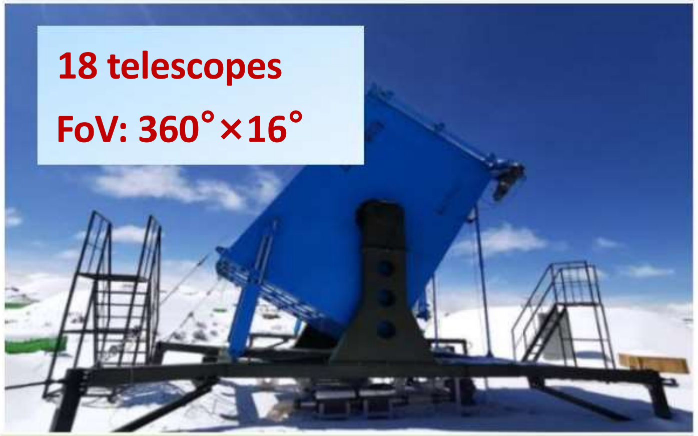

Very unique spectrometer of CR H, He and Fe above 30 TeV

KM2A: 1.36 $(km)^2$

- 5195 EDs
  - 1 m^2 each
  - 15 m spacing
- 1188 MDs
  - 36 m^2 each
  - 30 m spacing

Scintillator Detectors （ED）

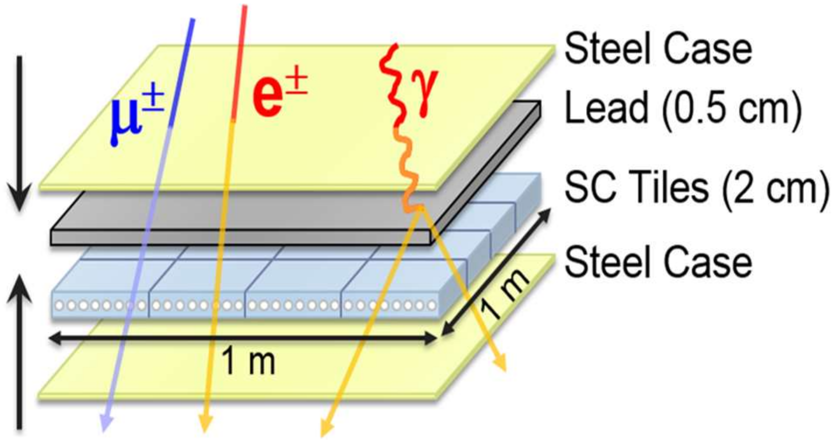

Muon detector（MD）

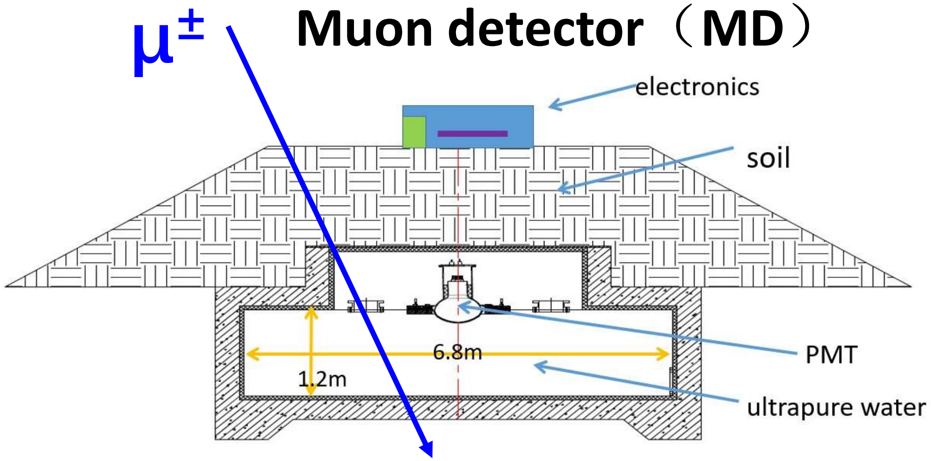

Inner View of one ED

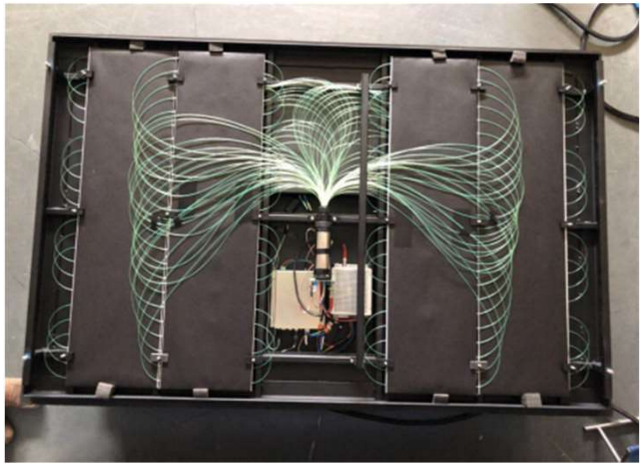

LHAASO-KM2A

Selection of γ–rays out of CR background

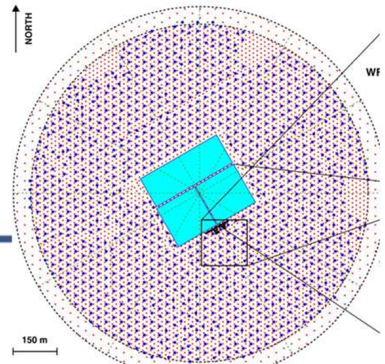

Active Area for Muons vs. Array Area: 4%

~1 PeV CR event: many muons ~ 1 PeV γ–ray event： very few muons

from the Crab

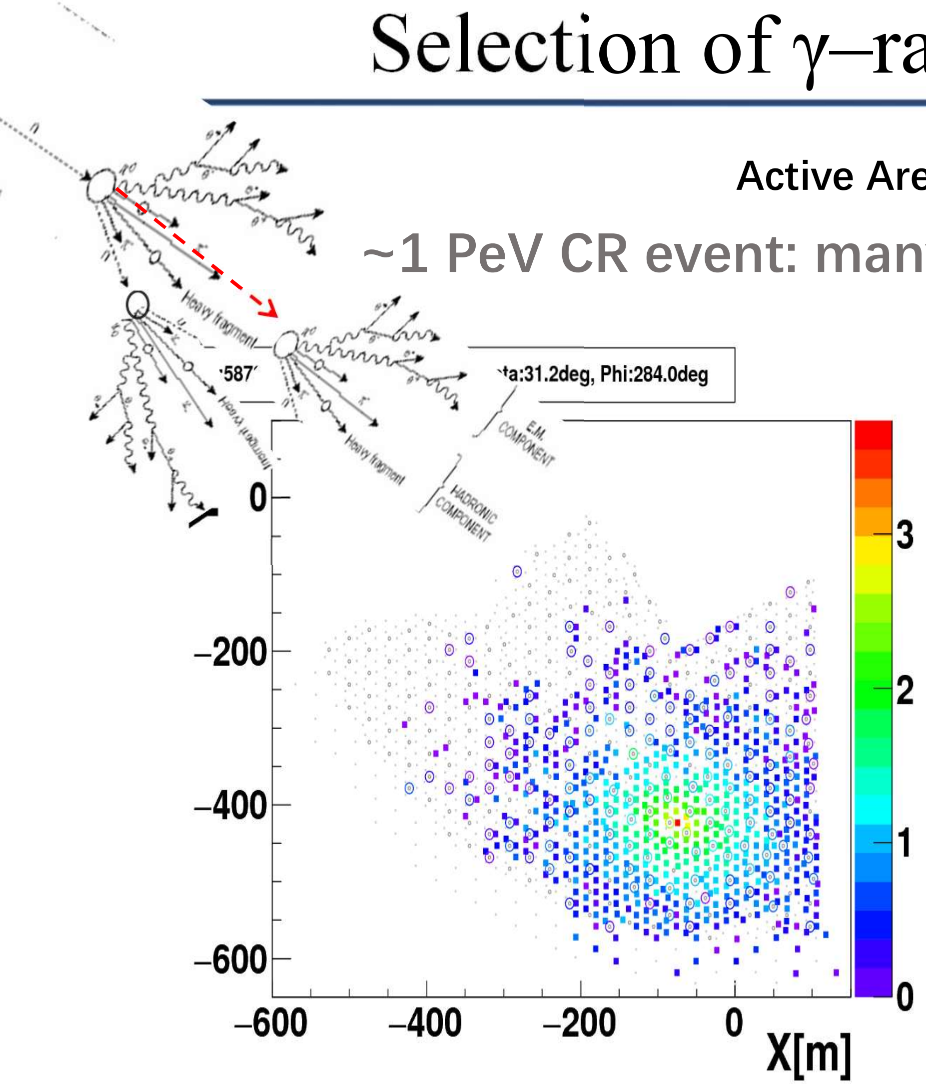

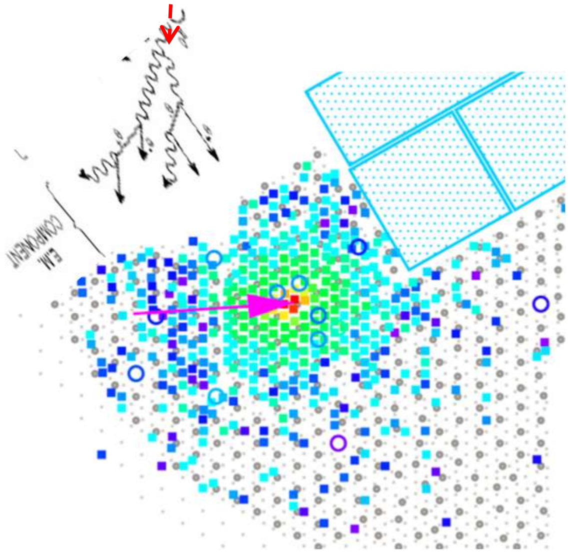

- Area：
  1.3 km^2
- Detectors：
  5216 ED
  1188 MD
- Energy Range：
  0.01-10 PeV

Water Cherenkov Detector Array (WCDA)

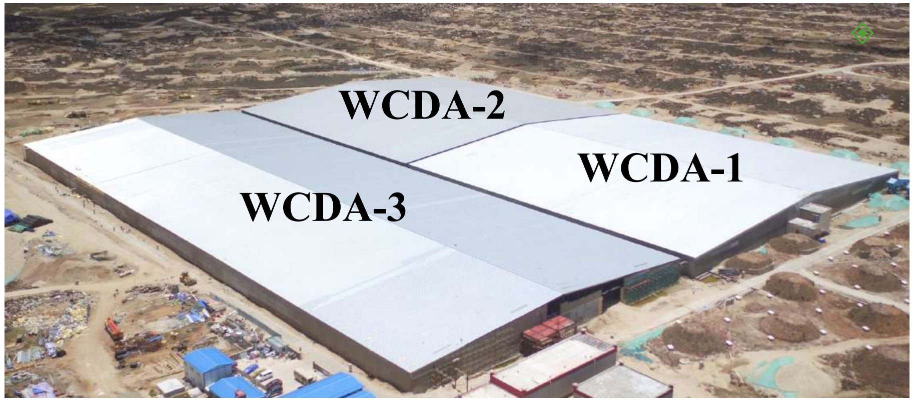

Energy rang

- WCDA-1
  - 300 GeV – 10 PeV
- WCDA-2 and WCDA-3
  - 100 GeV - 10 TeV

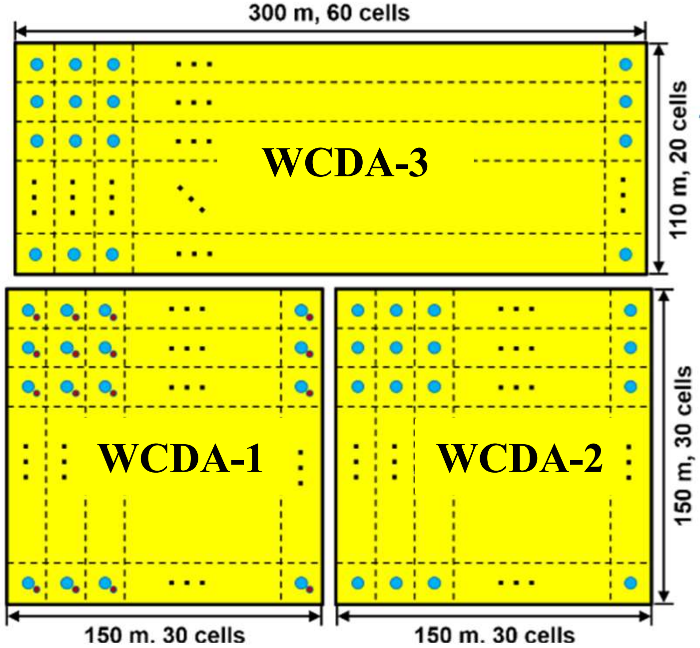

- Total area: $78,000m^2$
- Total units: 3,120
- Unit size: $5m \times 5m \times 4.4m$
- Two type of PMTs in each unit:
  - 8 inches and 1.5 inches for WCDA-1
  - 20 inches and 3 inches for WCDA-2 and WCDA-3

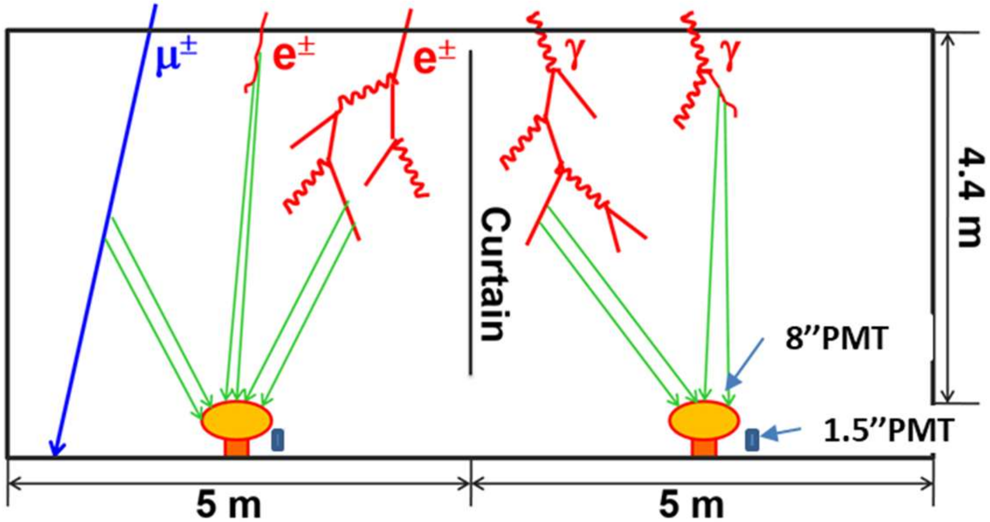

Inside of WCDA-3

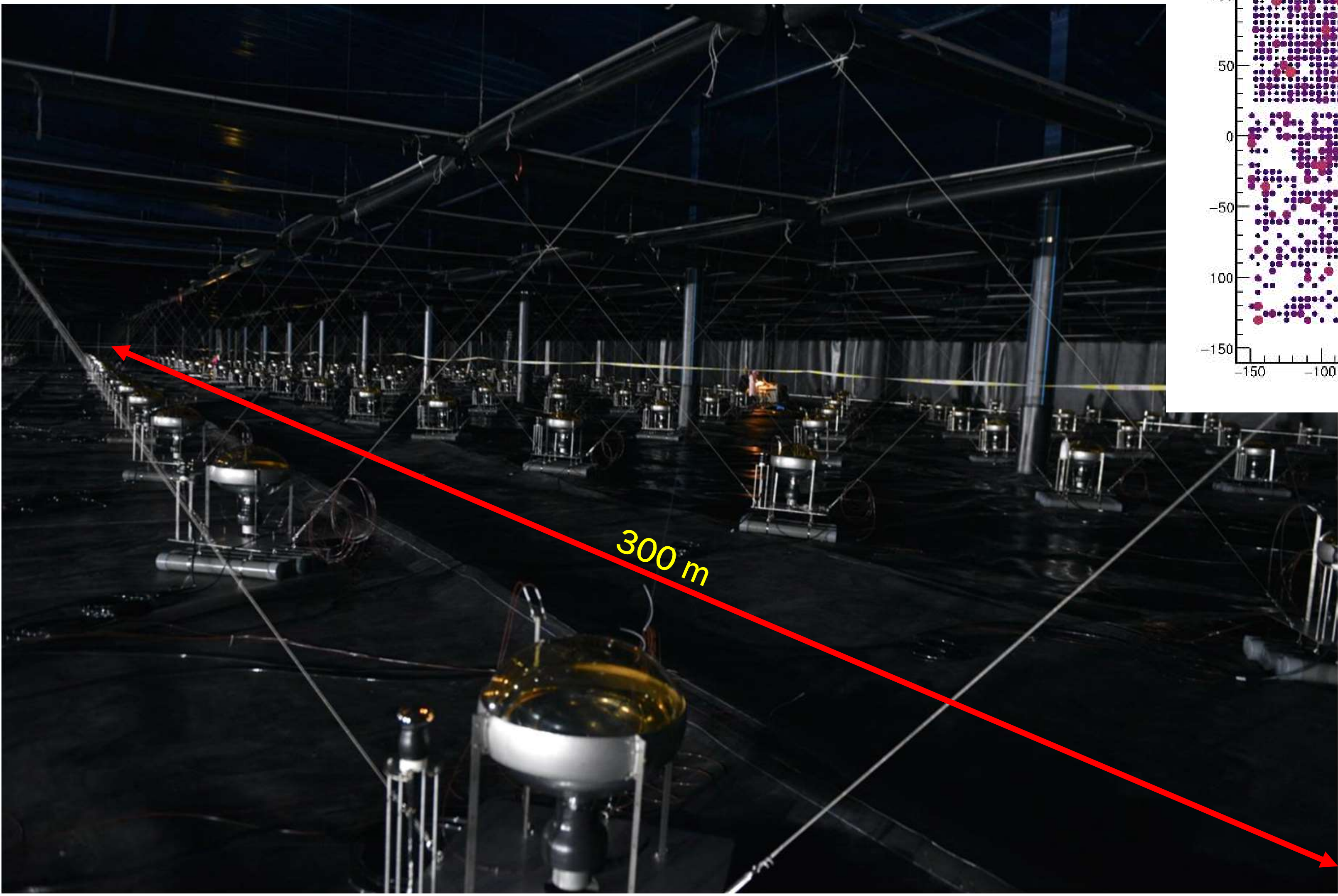

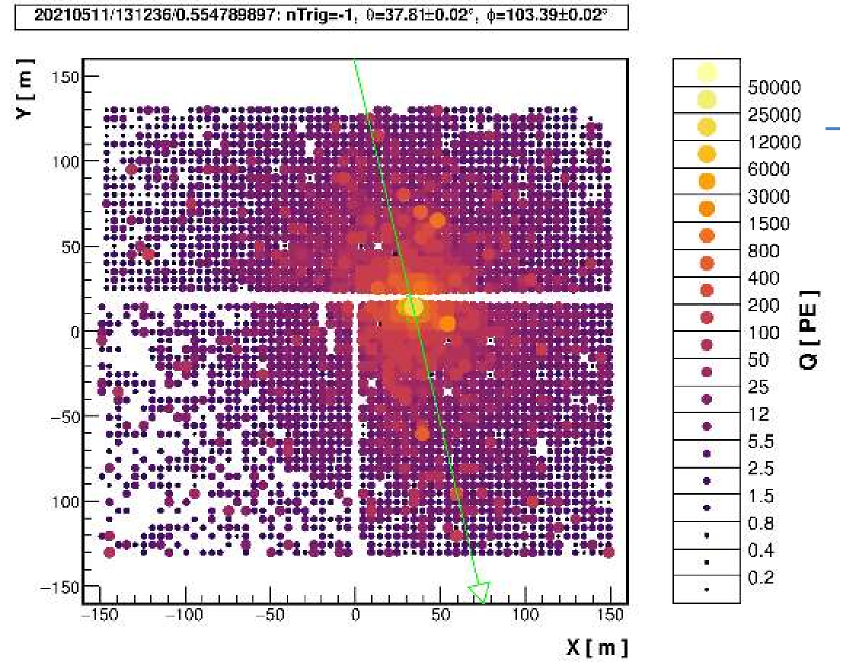

- WCDA-1 started operating in April 2019
- WCDA-2 started operating in January 2020
- WCDA-3 started operating in March 2021

Wide Field of View Cherenkov Telescope (WFCTA)

◆ Telescope parameters:

- ~5 m^2 spherical mirror
- Camera: 32×32 SiPMs array
- FOV: 16° × 16°
- Pixel size: 0.5°

Mirror

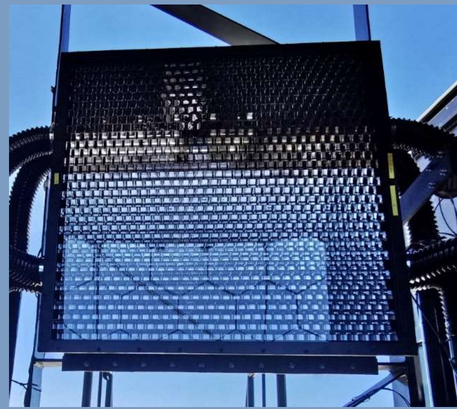

SiPM camera

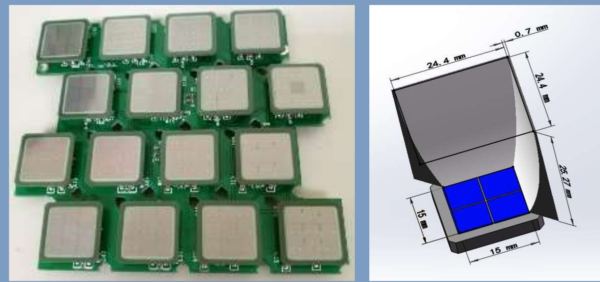

SiPM and Winstone cone